BACKSCATTER OF ULTRASONIC WAVES FROM A ROUGH LAYER

Technical Report EE-TR-4

Department of Electrical Engineering
Kansas State University
Manhattan, Kansas

MAY, 1966

KANSAS STATE UNIVERSITY
MANHATTAN, KANSAS

Technical Report EE-TR-4

BACKSCATTER OF ULTRASONIC WAVES FROM A ROUGH LAYER

By

Wu-Shi Shung

W. W. Koepsel

S. H. Durrani

Department of Electrical Engineering

MAY, 1966

This work was supported
partially by NsG 692 and
by a subcontract (through
University of Kansas) of
NASA contract #NSR-17-004-003

ABSTRACT

The backscatter from a rough surface is usually calculated by using Kirchhoff's approximation. In this report, the Kirchhoff's approximation is extended to the backscattering of an acoustic wave from a rough layer. The random rough interface of the layer is assumed to have one-dimensional Gaussian distributed surface heights.

Gaussian and exponential autocorrelation functions are used to represent the correlation of the heights at two different points. Expressions for the variance of the scattering coefficient are derived in the case that the rough side is very rough.

Experimental investigations were conducted at ultrasonic frequencies on a target designed to have Gaussian distribution and correlation. The measured variance of the scattering coefficient ρ, $D\{\rho\}$, has the following properties:

(A) $D\{\rho\}$ is highly frequency dependent; it decreases as the frequency increases.

(B) $D\{\rho\}$ decreases more rapidly than that obtained from a rough surface.

(C) The dependence of $D\{\rho\}$ on the incidence angle θ_1 is such that it increases as θ_1 increases, if θ_1 is small.

The experimental results lie between the theoretical results calculated for two kinds of correlation. This agrees with the measured value of the correlation function of the target.

Author

TABLE OF CONTENTS

1. INTRODUCTION. 1

2. EQUATIONS OF ACOUSTIC WAVE MOTION 2

2.1 Stresses, strains, and elastic constants. 2

2.2 The equations of motion. 5

2.3 General equations for damped waves 8

3. REFLECTION OF PLANE WAVE FROM A PLANE INTERFACE 10

3.1 Boundary conditions. 10

3.2 Reflection of waves at the interface of two isotropic and homogeneous media. 10

4. THE GENERAL KIRCHHOFF SOLUTION FOR SCATTERING FROM ROUGH SURFACES 15

4.1 General solution for surface with one-dimensional roughness. 15

4.2 Rough surface as random process. 22

4.3 Statistical distribution of the field. 25

4.4 The effect of absorption in the medium 26

4.5 Limitations of the general Kirchhoff method applied to acoustic wave scattering. 28

5. ACOUSTIC WAVE SCATTERING FROM LAYER 31

5.1 Layer with rough interface in the back 31

5.2 Layer with rough interface in the front. 36

5.3 Discussion of the derivation 49

6. EXPERIMENTAL WORK 51

6.1 Experimental set-up and procedure 51

6.2 Description of layer target. 55

6.3 Measurements and results 57

7. CONCLUSIONS 66

APPENDIX: EVALUATION OF INTEGRALS 67

REFERENCES. 69

LIST OF FIGURES

1. Reflection of plane wave at plane boundary. 12

2. Scattering from a rough surface 17

3. Local scattering geometry 17

4. Scattering from a layer with rough side in the back . . . 32

5. Transmission through a rough interface. 38

6. Scattering from a layer with rough side in the front. . . 42

7. Block-Diagram of experimental set-up. 52

8. The plexiglas with a one-dimensional rough surface. . . . 56

9. Variance of scattering coefficient of layer with rough side in the back 59

10. Variance of scattering coefficient of the rough surface of the layer. 60

11. Comparison of $D\{\rho\}$ from theoretical and experimental results.

    (a) $\theta_1=0^o$ 62

    (b) $\theta_1=5^o$ 63

    (c) $\theta_1=10^o$. 64

I. INTRODUCTION

The problem of the reflection of an acoustic plane wave from a plane interface separating two isotropic media has been solved by many physicists and geologists. Exact forms of the generated waves are given, related to the incidence angle and the acoustic impedances of the media. Brekhovskikh extended the work to deal with a layer having plane interfaces. The nature of wave scattered by a layer with rough interface, however, is generally unknown.

The backscattering of acoustic wave from a rough layer is analyzed in this report. The model of the layer considered contains a smooth interface in front and a random rough interface in back. The Kirchhoff's approximation for evaluating the scattering field of a rough surface (Beckmann 1963) is extended to deal with such a layer; experimental work has also been done for this model at different incidence angles and frequencies.

A tentative try is also made on the evaluation of backscatter from a layer with a very rough surface in the front. Equations are derived for this layer with no experimental support.

Owing to the analogies between acoustic and electromagnetic waves, the results of this work can be directly applied to the same problems in electromagnetic waves. The radar cross section is obtained just by modifying the variance of the scattering coefficient with a scaling factor. Application of the results can be found in the survey of lunar surface and in geological explorations.

II. EQUATIONS OF ACOUSTIC WAVE MOTION

2.1 Stresses, strains, and elastic constants

In an ideal isotropic homogeneous medium, a wave may propagate without any loss of amplitude due to internal friction. When the medium is defomable and undergoes a change in configuration due to the application of forces, the body is said to be strained. (Redwood 1960, Ewing 1957). It is assumed that a point P (X, y, z) is displaced, and the coordinates of the displacement are (u, v, w). An adjacent point Q(x+δx,y+δy,z+δz) is displaced by (u+δu,v+δv,w+δw). By Taylor's theorem, neglecting the higher terms under the assumption of small perturbation,

$$u + \delta u = u + \frac{\partial u}{\partial x}\delta x + \frac{\partial u}{\partial y}\delta y + \frac{\partial u}{\partial z}\delta z \quad ,$$

$$v + \delta v = v + \frac{\partial v}{\partial x}\delta x + \frac{\partial v}{\partial y}\delta y + \frac{\partial v}{\partial z}\delta z \quad , \qquad (2.1)$$

$$w + \delta w = w + \frac{\partial w}{\partial x}\delta x + \frac{\partial w}{\partial y}\delta y + \frac{\partial w}{\partial z}\delta z \quad .$$

The analysis may be simplified by writing

$$\frac{\partial u}{\partial x} = e_{xx} \quad , \quad \frac{\partial v}{\partial y} = e_{yy} \quad , \quad \frac{\partial w}{\partial z} = e_{zz} \quad ,$$

$$\frac{\partial v}{\partial x} + \frac{\partial u}{\partial y} = e_{xy} = e_{yx} \quad , \quad \frac{\partial u}{\partial z} + \frac{\partial w}{\partial x} = e_{zx} = e_{xz} \quad ,$$

$$\frac{\partial w}{\partial y} + \frac{\partial v}{\partial z} = e_{yz} = e_{zy} \quad , \qquad (2.2)$$

$$\frac{\partial v}{\partial x} - \frac{\partial u}{\partial y} = \omega_z \quad , \quad \frac{\partial u}{\partial z} - \frac{\partial w}{\partial x} = \omega_y \quad , \quad \frac{\partial w}{\partial y} - \frac{\partial v}{\partial z} = \omega_x \quad .$$

Then the displacements may be rewritten as

$$u+\delta u=u+(e_{xx}\delta x+\tfrac{1}{2}e_{xy}\delta y+\tfrac{1}{2}e_{xz}\delta z)+(\omega_y\delta z-\omega_z\delta y) \quad ,$$

$$v+\delta v=v+(\tfrac{1}{2}e_{yx}\delta x+e_{yy}\delta y+\tfrac{1}{2}e_{yz}\delta z)+(\omega_z\delta y-\omega_x\delta x) \quad , \qquad (2.3)$$

$$w+\delta w=w+(\tfrac{1}{2}e_{zx}\delta x+\tfrac{1}{2}e_{zy}\delta y+e_{zz}\delta z)+(\omega_x\delta y-\omega_y\delta x) \quad .$$

e_{xx}, e_{yy}, e_{zz} represent simple extensions of the medium in the vicinity of P (x, y, z);

e_{xy}, e_{yz}, e_{zx} represent the shear strains; and ω_x, ω_y, ω_z represent the rotation of the element as a rigid body.

To express the displacement in vector form

$$\vec{s} = u\vec{x}_o + w\vec{z}_o + v\vec{y}_o \quad , \qquad (2.4)$$

where $\vec{x}_o$, $\vec{y}_o$, and $\vec{z}_o$ are unit vectors in the directions of x-, y-, and z- axes, respectively.

For small perturbation, the shear strain is so small that it has no contribution to the volume change. Then the cubic dilatation Δ is defined as

$$\Delta = \lim_{\delta x,\delta y,\delta z\to 0} \frac{(\delta x+e_{xx}\delta x)(\delta y+e_{yy}\delta y)(\delta z+e_{zz}\delta z)-\delta x\delta y\delta z}{\delta x\delta y\delta z} \qquad (2.5)$$

$$= e_{xx} + e_{yy} + e_{zz}$$

$$= \text{div } \vec{s} \quad ,$$

and the rotational displacement $\vec{\omega}$ becomes

$$\vec{\omega} = \omega_x \vec{x}_o + \omega_y \vec{y}_o + \omega_z \vec{z}_o$$

$$= \frac{1}{2} \text{curl } \vec{s} \quad . \tag{2.6}$$

To discuss the force acting on an element of volume in a medium, nine components of stress, which have the units of force/area, are required. Let the stresses be denoted by τ_{ij}, where the first subscript is associated with the axis normal to the place on which the stress acts, and the second subscript to the direction of the stress. In an isotropic homogeneous medium, there are only two elastic constants, Lame's constants λ and μ, to relate the stress and strain together. In the case of ideal fluid and ideal gas $\mu = 0$. The stress and strain relations by Lame are as follows:

$$\begin{aligned}
&\tau_{xx} = \lambda(e_{xx}+e_{yy}+e_{zz}) + 2\mu e_{xx} = \lambda\Delta + 2\mu e_{xx} \quad , \\
&\tau_{yy} = \lambda(e_{xx}+e_{yy}+e_{zz}) + 2\mu e_{yy} = \lambda\Delta + 2\mu e_{yy} \quad , \\
&\tau_{zz} = \lambda(e_{xx}+e_{yy}+e_{zz}) + 2\mu e_{zz} = \lambda\Delta + 2\mu e_{zz} \quad , \\
&\tau_{xy} = \tau_{yx} = \mu e_{xy} = \mu e_{yx} \quad , \\
&\tau_{yz} = \tau_{zy} = \mu e_{yz} = \mu e_{zy} \quad , \\
&\tau_{zx} = \tau_{xz} = \mu e_{zx} = \mu e_{xz} \quad .
\end{aligned} \tag{2.7}$$

From (2.7), other elastic constants can be derived as follows, (Lamb 1925):

(a). Uniform stress and dilatation, $\tau_{xx}=\tau_{yy}=\tau_{zz}$, and

$$\tau_{xx}=\tau_{yy}=\tau_{zz}=(\lambda+\frac{2}{3}\mu)\Delta=k\Delta$$

$k=(\lambda+\frac{2}{3}\mu)$ is the compressibility.

(b). Shear stress τ_{xy} as defined by Eq. (2.7)

$$\mu = \frac{\tau_{xy}}{e_{xy}} = \frac{\tau_{yz}}{e_{yz}} = \frac{\tau_{zx}}{e_{zx}}$$

is the coefficient of rigidity.

(c). Longitudinal stress, $\tau_{yy}=\tau_{zz}=0$,

$$\tau_{xx} = \frac{\mu(3\lambda+2\mu)}{\lambda+\mu} e_{xx} = Ee_{xx} ,$$

E is the Young's Modulus.

(d). Poisson's ratio, σ , represents the ratio of lateral contraction to longitudinal extension. In this case,

$\tau_{yy} = \tau_{zz} = 0$, $e_{yy} = e_{zz} = \sigma e_{xx}$, and $\sigma = \frac{\lambda}{2(\lambda+\mu)}$.

The constants λ, μ, k can be expressed in terms of Young's Modulus and Poisson's Radio:

$$\lambda = \text{Lame's constant} = \frac{\sigma E}{(1+\sigma)(1-2\sigma)} ,$$

$$\mu = \text{Rigidity} = \frac{E}{2(1+\sigma)} , \qquad (2.8)$$

$$k = \text{Compressibility} = \frac{E}{3(1-2\sigma)} .$$

2.2 The equations of motion

According to Newton's equation of motion, the x-component of the resultant force on the volume element is

$$(\rho \delta x \cdot \delta y \delta z)\frac{\partial^2 u}{\partial t^2} = (\tau_{xx} + \frac{\partial \tau_{xx}}{\partial x}\,\delta x - \tau_{xx})\,\delta y \delta z$$

$$+ (\tau_{yx} + \frac{\partial \tau_{yx}}{\partial y}\cdot \delta y - \tau_{yx})\,\delta z \delta x$$

$$+ (\tau_{zx} + \frac{\partial \tau_{zx}}{\partial z}\,\delta z - \tau_{zx})\,\delta x \delta y \quad ,$$

$$\text{or,} \qquad \rho\,\frac{\partial^2 u}{\partial t^2} = \left(\frac{\partial \tau_{xx}}{\partial x} + \frac{\partial \tau_{yx}}{\partial y} + \frac{\partial \tau_{zx}}{\partial z}\right) \quad ,$$

where ρ is the density of the medium. For an isotropic homogeneous medium, Equation (2.7) holds, giving

$$\rho\,\frac{\partial^2 u}{\partial t^2} = \frac{\partial}{\partial x}\,(\lambda\Delta + 2\mu e_{xx}) + \frac{\partial}{\partial y}\,(\mu e_{yx}) + \frac{\partial}{\partial z}\,(\mu e_{zx})$$

$$= (\lambda+2\mu)\,\frac{\partial \Delta}{\partial x} - 2\mu\left(\frac{\partial \omega_z}{\partial y} - \frac{\partial \omega_y}{\partial z}\right) \quad .$$

Similar arguments apply to the y-, and z- components, so that

$$\rho\,\frac{\partial^2 \vec{s}}{\partial t^2} = (\lambda+2\mu)\ \text{grad}\ \Delta - 2\mu\ \text{curl}\ \vec{\omega} \quad . \tag{2.9}$$

Equation (2.9) is the equation of motion in an isotropic medium. It is usually rewritten in the form of displacement potentials ϕ and $\vec{\psi}$ by the following transformations

$$\vec{s} = -\ (\text{grad}\ \phi \bullet \text{curl}\ \vec{\psi}) \quad , \tag{2.10}$$

$$\text{div}\ \vec{\psi} = 0 \quad .$$

Substituting (2.10) into (2.9),

$$\rho\frac{\partial^2}{\partial t^2}(\text{grad }\phi+\text{curl}\vec{\psi})=(\lambda+2\mu)\text{grad}(\nabla^2\phi)-\mu\text{curl}(\text{curlcurl}\vec{\psi}),$$

$$\rho\frac{\partial^2}{\partial t^2}(\text{grad}\phi+\text{curl}\vec{\psi})=(\lambda+2\mu)\text{grad}(\nabla^2\phi)+\mu\text{curl}(\nabla^2\vec{\psi}), \qquad (2.11)$$

where ∇^2 denotes the Laplacian, defined by $\nabla^2\phi$ = Div. Grad ϕ for a scalar ϕ, and $\nabla^2\vec{\psi}$ = Grad Div $\vec{\psi}$-curl curl $\vec{\psi}$ for a vector $\vec{\psi}$. In the cartesian coordinate system,

$$\nabla^2=\frac{\partial^2}{\partial x^2}+\frac{\partial^2}{\partial y^2}+\frac{\partial^2}{\partial z^2}.$$

By taking the divergence and curl on Equation (2.11) the scalar and vector potentials can be separated:

$$\frac{\partial^2\phi}{\partial t^2}=C_\ell{}^2\nabla^2\phi\ ,\ C_\ell{}^2=\frac{\lambda+2\mu}{\rho}\ ; \qquad (2.12)$$

$$\frac{\partial^2\vec{\psi}}{\partial t^2}=C_s{}^2\nabla^2\vec{\psi}\ ,\ C_s{}^2=\frac{\mu}{\rho}\ . \qquad (2.13)$$

In Equation (2.11) and (2.12), the scalar displacement potential ϕ travels with velocity C_ℓ and involves no rotation; it is called "longitudinal", or "compressional", or "dilatational" or "irrotational", or "P-Wave"; the vector displacement potential $\vec{\psi}$ travels with velocity C_s and involves rotation; it is called "shear", or "transverse", or "lateral", or "equivoluminal", or "rotational", or "distortional", or "S-Wave". The names Longitudinal and Shear waves shall be used throughout this report.

In ideal gases and fluids, the ordinary acoustic wave initiates a wave motion in which the sign of dilatation changes very fast so that there is no time for sensible transfer of heat between adjacent portions of the medium. The flow of heat hardly sets in from one element to another before its direction is reversed, and the conditions are practically adiabatic. Moreover, since $\mu = o$, no shear wave propagates in an ideal gas or fluid. The Lame's constant λ for an ideal gas is found to be

$$\lambda = K_{ad} = \lambda P_o \qquad (2.14)$$

K_{ad}: adiabatic compressibility,

λ : (specific heat at constant volume)/(specific heat at constant pressure),

P_o : gas pressure.

In an ideal fluid, $\lambda = K_{ad}$ is usually influenced by many factors. λ is related to the longitudinal wave velocity C_ℓ by $C_\ell = \sqrt{\lambda/\rho}$, and an empirical equation giving C_ℓ in water is

$$C_\ell = 141{,}000+4.21t-3.7t^2+110s+0.018d, \qquad (2.15)$$

C_ℓ = longitudinal wave velocity (cm/sec),

t = temperature (C),

s = salinity (1/1000 in weight),

d = depth (cm).

2.3 General equation for damped waves

The dissipative forces in acoustic wave motion are proportional to the velocity of the particles in the medium for small perturbations. The force of the elastic stress must both accelerate the medium and overcome the dissipative forces, so the equations of motion, Equations (2.11) and (2.12), are modified (Kinsler and Frey 1950) as follows:

$$\frac{\partial^2 \phi}{\partial t^2} + \frac{\eta}{\rho} \frac{\partial \phi}{\partial t} = C_\ell{}^2 \nabla^2 \phi \,, \tag{2.16}$$

$$\frac{\partial \vec{\psi}}{\partial t^2} + \frac{\eta}{\rho} \frac{\partial \vec{\psi}}{\partial t} = C_s{}^2 \nabla^2 \vec{\psi} \,, \tag{2.17}$$

where η has the unit of $\frac{(\text{mass})\ (\text{time})^{-1}}{(\text{volume})}$

The general solution of Equations (2.16) and (2.17) has the usual form $E = Ae^{i(\lambda . r - \omega t)}$, where r is the distance from certain reference point. Substituting into Equations (2.16) or (2.17), the propagation constant λ is found to be

$$\lambda = K + i\alpha$$

where

$K = \omega/C$ is the wave number,

$\alpha = \eta/2\rho C$ is the attenuation constant.

For water at room temperature, the attenuation constant is about one thousandth of the value of air. For this reason, ultrasonics are very well suited for underwater signal transmission as opposed to the case in air. As for the possible shear waves transmission in viscous gas and liquid, the skin depth is found to be $\sqrt{2\xi/\rho\omega}$, where ξ is the shear viscosity.

These waves behave very much like electromagnetic waves penetrating a metal. For water at 1 mc, the skin depth is only 5.6×10^{-5}cm. In most cases, shear wave propagation can be neglected in gases and liquid.

3. REFLECTION OF PLANE WAVE FROM A PLANE INTERFACE

3.1 Boundary conditions

The continuity of normal and tangential components of displacements and stresses across the interface give the following boundary conditions (Brekhovskikh 1960):

$$\begin{aligned}
&\vec{n} \cdot (\vec{s}_1 - \vec{s}_2) = o \ ; \\
&\vec{n} \times (\vec{s}_1 - \vec{s}_2) = o \ ; \\
&\vec{n} \cdot (\vec{\tau}_1 - \vec{\tau}_2) = o \ ; \\
&\vec{n} \times (\vec{\tau}_1 - \vec{\tau}_2) = o \ .
\end{aligned} \qquad (3.1)$$

Taking the z-axis as the normal to the plane, Equation (3.1) can be expressed in terms of displacement potentials ϕ and $\vec{\psi}$ as,

$$\vec{n} \cdot \vec{s} = w = -\left(\frac{\partial \phi}{\partial z} + \frac{\partial \psi_y}{\partial x} - \frac{\partial \psi_x}{\partial y}\right) \ ;$$

$$\vec{n} \times \vec{s} = -u\vec{x}_o + v\vec{y}_o = \left(\frac{\partial \phi}{\partial x} + \frac{\partial \psi_z}{\partial y} - \frac{\partial \psi_y}{\partial z}\right) \vec{x}_o + \left(-\frac{\partial \phi}{\partial y} - \frac{\partial \psi_x}{\partial z} + \frac{\partial \psi_z}{\partial x}\right) \vec{y}_o \ ;$$

$$n \cdot \tau = \tau_{zz} = \omega^2 \left[\rho \phi + \frac{2\rho}{K_s^2} \left(\frac{\partial^2 \phi}{\partial x^2} + \frac{\partial^2 \psi_y}{\partial z \partial x} + \frac{\partial^2 \psi_x}{\partial z \partial y} + \frac{\partial^2 \phi}{\partial y^2} \right) \right] \ ;$$

$$\begin{aligned}
\vec{n} \times \vec{\tau} &= -\tau_{zx}\vec{x}_o + \tau_{zy}\vec{y}_o \\
&= \mu \left(2 \frac{\partial^2 \phi}{\partial x \partial z} + \frac{\partial^2 \psi_z}{\partial y \partial z} - \frac{\partial^2 \psi_z}{\partial z^2} + \frac{\partial^2 \psi_y}{\partial x^2} - \frac{\partial^2 \psi_x}{\partial x \partial y} \right) \vec{x}_o \\
&\quad - \mu \left(2 \frac{\partial^2 \phi}{\partial y \partial z} + \frac{\partial^2 \psi_y}{\partial y \partial z} - \frac{\partial^2 \psi_x}{\partial y^2} + \frac{\partial^2 \psi_x}{\partial z^2} - \frac{\partial^2 \psi_z}{\partial z \partial x} \right) \vec{y}_o \ .
\end{aligned}$$

3.2 Reflection of waves at the interface of two isotropic and homogeneous media

Let A, B, and D represent the amplitudes of the potential of incident, reflected, and transmitted waves, where the subscripts

ℓ and s denoting longitudinal and shear wave (Fig. 1). According to Huygen's principle, the phase velocities for each wave are equal at the boundary, therefore,

$$K_{1\ell}=|\vec{K}_{1\ell}|=K'_{1\ell}=|\vec{K}_{1\ell}| \quad , \quad K_{1s}=|K_{1s}|=K'_{1s}=|K'_{1s}|$$

$$C_p = \frac{C_{1\ell}}{\sin\theta_1} = \frac{C_{1s}}{\sin\gamma_1} = \frac{C_{1\ell}}{\sin\theta'_1} = \frac{C_{1s}}{\sin\gamma'_1} = \frac{C_{2\ell}}{\sin\theta_2} = \frac{C_{2s}}{\sin\gamma_2}$$

$$\theta_1 = \theta'_1 \quad , \quad \gamma_1 = \gamma'_1 \quad . \tag{3.2}$$

It is shown that the longitudinal or vertically polarized wave, $\vec{\psi} = \vec{\psi}_y \vec{y}_o$, is always reflected and transmitted in the modes of longitudinal and vertically polarized shear waves (Brekhovskikh, 1960). In other words, the vector displacements potentials involved can always be assumed to be in the direction of the y-axis and independent of y. The potentials in media #1 and #2 are assumed as follows:

$$\phi_1=A_\ell \cdot \exp\,[iK_{1\ell}(x\sin\theta_1+z\cos\theta_1)] + B_\ell \cdot \exp\,[iK_{1\ell}(x\sin\theta_1 - z\cos\theta_1)],$$

$$\vec{\psi}_1=A_s \cdot \exp\,[iK_{1s}(x\sin\gamma_1+z\cos\gamma_1)]\vec{y}_o+B_s \cdot \exp\,[iK_{1s}(x\sin\gamma_1-z\cos\gamma_1)]\vec{y}_o$$

$$\phi_2=D_\ell \exp\,[iK_{2\ell}(x\sin\theta_2+z\cos\theta_2)],$$

$$\vec{\psi}_2=D_s \exp\,[iK_{2s}(x\sin\gamma_2+z\cos\gamma_2)]. \tag{3.3}$$

The boundary conditions at z=0 are

$$\frac{\partial\phi_1}{\partial z} + \frac{\partial\psi_{1y}}{\partial x} = \frac{\partial\phi_2}{\partial z} + \frac{\partial\psi_{2y}}{\partial x} \tag{3.4}$$

$$\frac{\partial\phi_1}{\partial x} - \frac{\partial\psi_{1y}}{\partial z} = \frac{\partial\phi_2}{\partial x} - \frac{\partial\psi_{2y}}{\partial z} \tag{3.5}$$

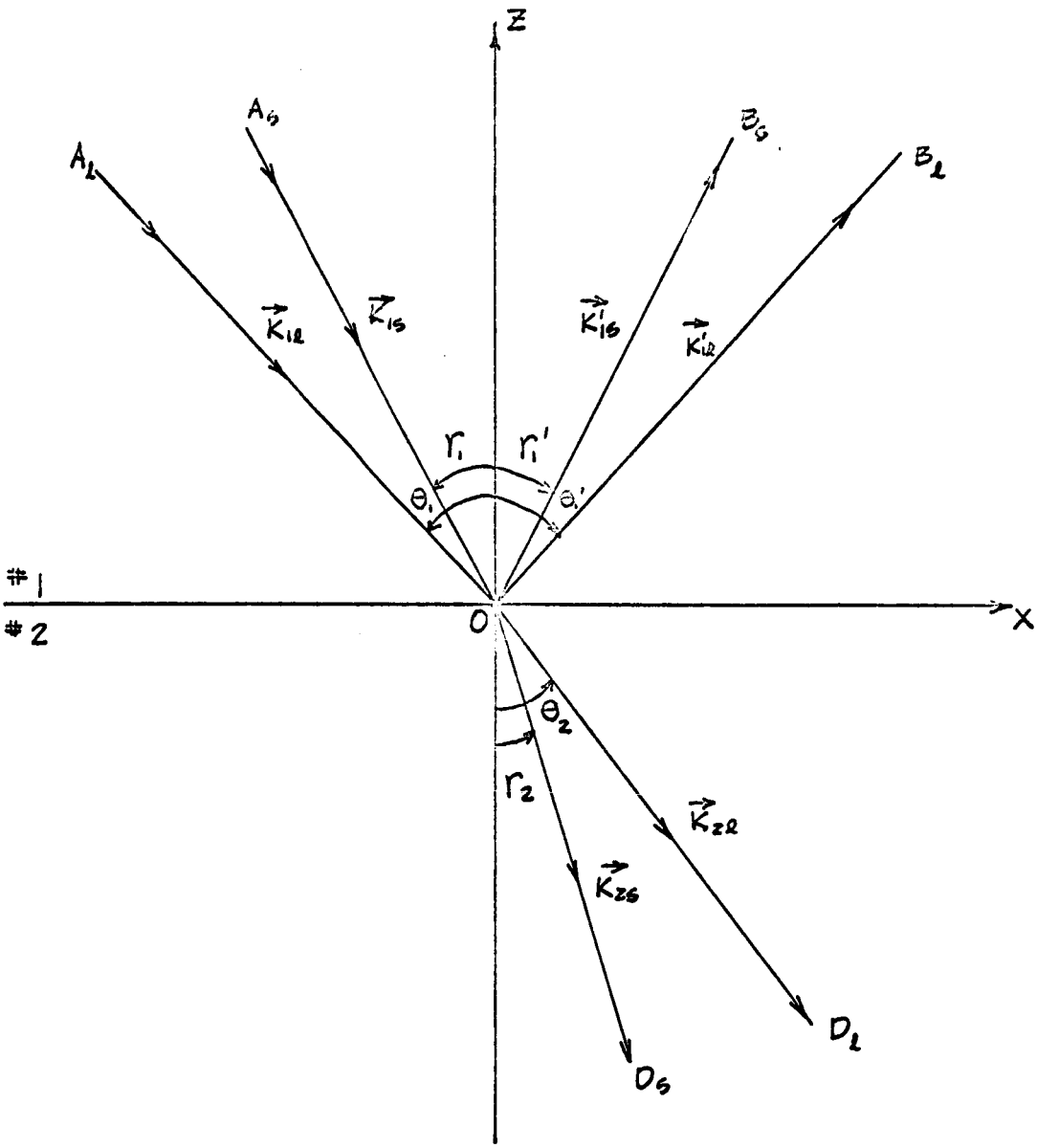

FIG.1. REFLECTION OF PLANE WAVE AT PLANE BOUNDARY

$$\rho_1\phi_1 + \frac{2\rho_1}{K_{1s}^2}\left(\frac{\partial^2\phi_1}{\partial x^2} - \frac{\partial^2\psi_{1y}}{\partial x\partial z}\right) = \rho_2\phi_2 + \frac{2\rho_2}{K_{2s}^2}\left(\frac{\partial^2\phi_2}{\partial x^2} - \frac{\partial^2\psi_{2y}}{\partial x\partial z}\right) ; \qquad (3.6)$$

$$2\mu_1\frac{\partial\phi}{\partial x\partial z} + \mu_1\left(\frac{\partial^2\psi_{1y}}{\partial x^2} - \frac{\partial^2\psi_{1y}}{\partial z^2}\right) = 2\mu_2\frac{\partial^2\phi_2}{\partial x\partial z} + \mu_2\left(\frac{\partial^2\psi_{2y}}{\partial x^2} - \frac{\partial^2\psi_{2y}}{\partial z^2}\right) . \qquad (3.7)$$

Upon substituting Equation (3.3) into Equations (3.4), (3.5), (3.6) and (3.7), the boundary conditions are expressed in terms of potentials as follows:

$$(A_\ell - B_\ell)K_{1\ell}\cos\theta_1 + (A_s + B_s)K_{1s}\sin\gamma_1 = D_\ell K_{2\ell}\cos\theta_2 + D_s K_{2s}\sin\gamma_2 , \qquad (3.8)$$

$$(A_\ell + B_\ell)K_{1\ell}\sin\theta_1 - (A_s - B_s)K_{1s}\cos\gamma_1 = D_\ell K_{2\ell}\sin\theta_1 - D_s K_{2s}\cos\gamma_2 ; \qquad (3.9)$$

$$\rho_1(A_\ell + B_\ell)\left(1 - 2\frac{K_{1\ell}^2}{K_{1s}^2}\sin^2\theta_1\right) + \rho_1(A_s - B_s)\sin 2\gamma_1 = \rho_2 D_\ell\left(1 - 2\frac{K_{2\ell}^2}{K_{2s}^2}\sin^2\theta_2\right) + \rho_2 D_s\sin 2\gamma_2 \qquad (3.10)$$

$$\rho_1(A_\ell - B_\ell)\frac{K_\ell^2}{K_{1s}^2}\sin 2\theta_1 - \rho_1(A_s + B_s)\cos 2\gamma_1 = \rho_2 D_\ell\frac{K_2}{K_{2s}^2}\sin\theta_2 - \rho_2 D_s\cos 2\gamma_2 . \qquad (3.11)$$

By setting A_s, or A_ℓ equal to zero, corresponding to longitudinal or shear wave incidence, respectively, the amplitude of the generated waves can be expressed in terms of the amplitude of the the incident wave potential. It is to be noted that when the incident angle is small, all the sinusoidal term tends to the limits 1 and 0. Then the boundary condition is further simplified to

$$(A_\ell - B_\ell)K_{1\ell} = D_\ell K_{2\ell} , \qquad (3.12)$$

$$-(A_s-B_s)K_{1s}=-D_sK_{2s} \; ; \tag{3.13}$$

$$-\rho_1(A_\ell+B_\ell)=\rho_2 D_\ell \; ; \tag{3.14}$$

$$-\rho_1(A_s+B_s)=-\rho_s D_s \; . \tag{3.15}$$

Solving Equations (3.12), (3.13), (3.14), and (3.15)

$$\frac{B_\ell}{A_\ell}=\frac{\rho_2 C_{z\ell}-\rho_1 C_{1\ell}}{\rho_2 C_{2\ell}+\rho_1 C_{1\ell}} \; , \quad \frac{D_\ell}{A_\ell}=\frac{2\rho_2 C_{2\ell}}{\rho_2 C_{2\ell}+\rho_1 C_{1\ell}}\cdot\frac{\rho_1}{\rho_2} \; ; \tag{3.16}$$

$$\frac{B_s}{A_s}=\frac{\rho_2 C_{2s}-\rho_1 C_{1s}}{\rho_s C_{2s}+\rho_1 C_{1s}} \; , \quad \frac{D_s}{A_s}=\frac{2\rho_2 C_{2s}}{\rho_2 C_{2s}+\rho_1 C_{1s}}\cdot\frac{\rho_1}{\rho_2} \; . \tag{3.17}$$

Equations (3.16) and (3.17) imply that when the angle of incidence is small, no change of mode occurs at the interface of acoustic wave motion. This is a very important limitation in the acoustic simulation problem. The angle of incidence has to be very small if change of mode is to be avoided in the experiment.

4. THE GENERAL KIRCHHOFF SOLUTION FOR SCATTERING FROM ROUGH SURFACES

4.1 General solution for surface with one dimensional roughness

Beckmann (Beckmann, 1963) has derived the solution for the mean scattered field, power, and the statistical distribution of those quantities by the Kirchhoff approximation method. The principal limit of the approximation is that the surface must not contain a large amount of sharp edges, sharp points or other irregularities with small radii of curvature. The criterion for the validity of the approximation is given as

$$4Kr_c\cos\theta >> \lambda ,$$

where r_c is the radius of curvature, θ is the local angle of incidence, and λ is the wavelength of the wave.

The rough surface is given by the function

$$\xi = \xi(x) \tag{4.1}$$

with mean level coinciding with the plane

$$z = 0 . \tag{4.2}$$

The medium in the space $z>\xi(x)$ is assumed to be isotropic in which a monochromatic plane longitudinal wave

$$E_1 = e^{ik_1 \cdot r - i\omega t} \tag{4.3}$$

is transmitted, where

$$\vec{K}_1 = \frac{2\pi}{\lambda} \cdot \frac{\vec{K}_1}{K_1} \tag{4.4}$$

is the wave number of the incident wave, which is assumed to lie in the xz-plane (Fig. 2), and $\vec{r}$ is the radius vector

$$\vec{r} = x\vec{x}_o + \xi(x)\vec{z}_o . \tag{4.5}$$

The angle of incidence is denoted by θ_1, the scattering angle by θ_2, where the magnitude of k_2 and k_1 are equal:

$$|\vec{K}_2| = |\vec{K}_1| = K = \frac{2\pi}{\lambda} . \tag{4.6}$$

$\vec{K}_2$ also lies in the xz-plane for a one-dimensional rough scattering surface.

In order to deal with plane scattered waves, the observation point P is removed to the Fraunhofer zone of diffraction, $R' \to \infty$, where R' is the distance from P to a point $B(x,\xi(x))$ on the rough surface (Fig. 2). In other words,

$$K_2 R' = K_2 R_o - \vec{K}_z \cdot \vec{r} , \tag{4.7}$$

where R_o is the distance of P from the origin. The scattered potential E_2 at P is given by the Helmholtz integral

$$E_2(P) = \frac{1}{4\pi} \iint_S (E \frac{\partial \psi}{\partial \eta} - \psi \frac{\partial}{\partial \eta}) ds, \tag{4.8}$$

where

$$\psi = \frac{e^{iKR'}}{R'} \doteq \frac{e^{iKR_o - i\vec{K}_z \cdot \vec{r}}}{R_o} . \tag{4.9}$$

E and $\frac{\partial E}{\partial \eta}$ are the potential and its normal derivative on the rough surface S. The values of those two quantities are approximated in the Kirchhoff method by the value that would exist on the tangent plane at that point, i. e.,

$$(E)_s = (1+R) E_1 , \tag{4.10}$$

$$(\frac{\partial E}{\partial \eta})_s = i(1-R) E_1 \vec{K}_1 \cdot \vec{n} , \tag{4.11}$$

n is the normal to the surface at the considered point B (Fig. 3) and R is the longitudinal wave reflection coefficient of a smooth plane.

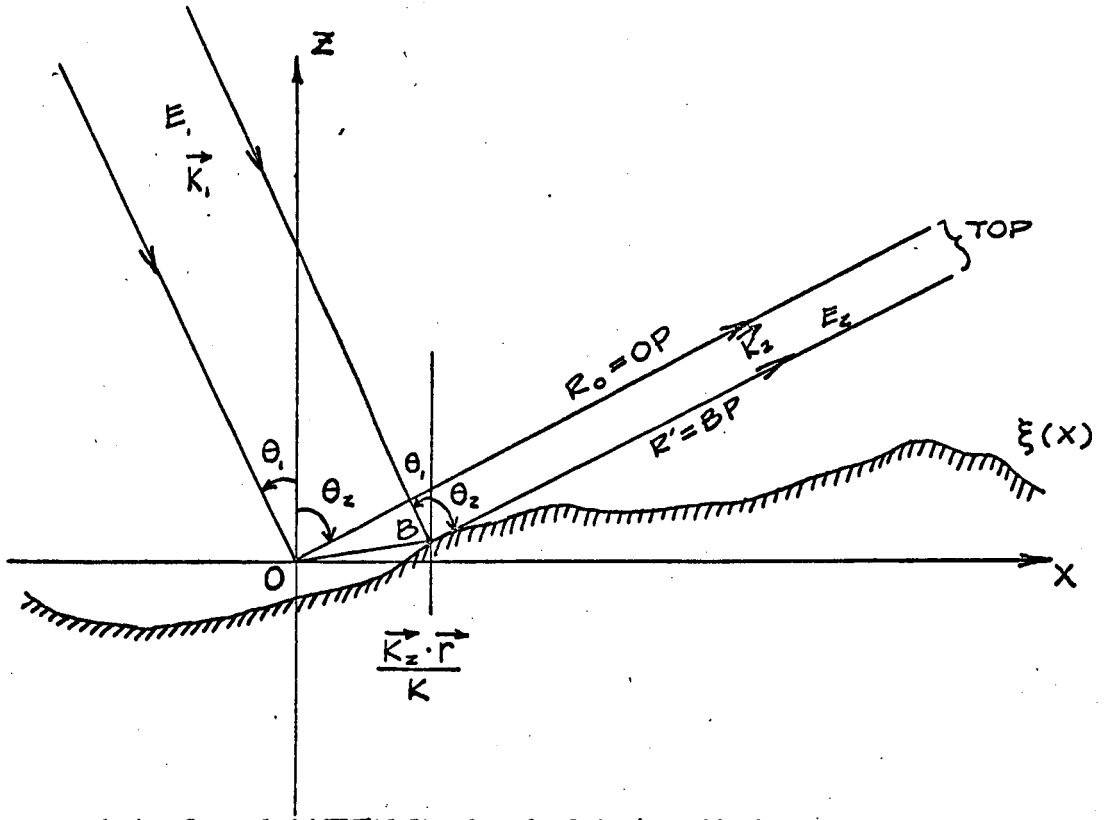

FIG. 2 . SCATTERING FROM A ROUGH SURFACE

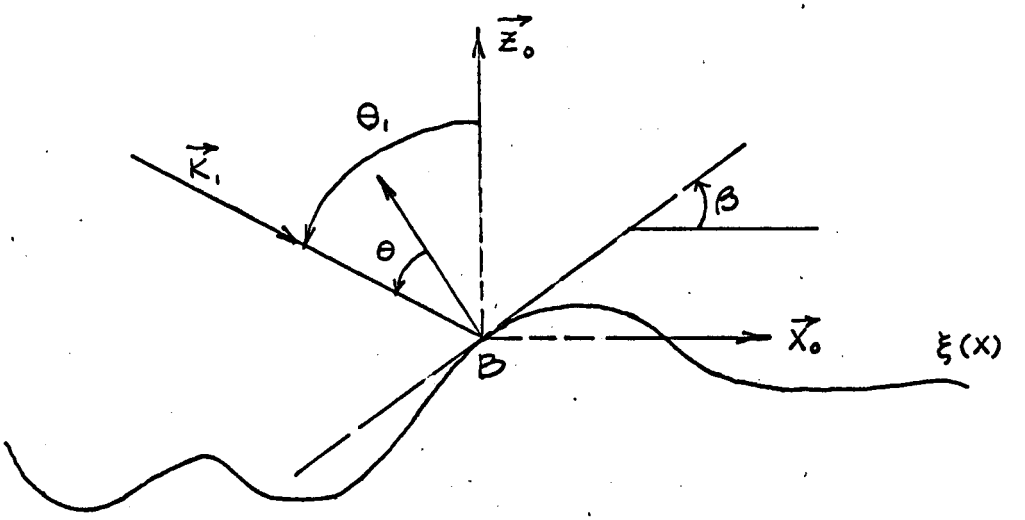

FIG. 3. LOCAL SCATTERING GEOMETRY

Then

$$\theta = \theta_1 - \beta = \theta_1 - \text{arc tan}\xi'(x) \ . \qquad (4.12)$$

Substituting Equations (4.9), (4.10), and (4.11) in (4.8),

$$E_2(P) = \frac{1}{4\pi}\iint_s (1+R)E_1(-i\ K_2\ n) - i\Psi(1-R)E_1\vec{K}_1\cdot\vec{n}\ \ ds$$

$$= \frac{1}{4\pi}\iint_s e^{i(\vec{K}_1-\vec{K}_2)\cdot\vec{r}-}\ R(\vec{K}_1-\vec{K}_2)-(\vec{K}_1+\vec{K}_2)\ \cdot\vec{n}\ ds,$$

or

$$E\ (P) = ie\frac{iK_2R_o}{4\pi R_o}\iint_s (R\vec{v}-\vec{P})e^{i\vec{v}\cdot\vec{r}}.\vec{n}ds \qquad (4.13)$$

where

$$\vec{K}_1 = K(\sin\theta_1\vec{x}_o - \cos\theta_1\vec{z}_o),$$

$$\vec{K}_2 = K(\sin\theta_2\vec{x}_o + \cos\theta_2\vec{z}_o),$$

$$\vec{n} = -\sin\beta\vec{x}_o + \cos\beta\vec{z}_o,$$

$$\vec{r} = x\vec{x}_o + \xi(x)\vec{z}_o,$$

$$\vec{v} = \vec{K}_1 - \vec{K}_2$$

$$= K(\sin\theta_1 - \sin\theta_2)\vec{x}_o - K(\cos\theta_1 + \cos\theta_2)\vec{z}_o$$

$$= v_x\vec{x}_o + v_z\vec{z}_o \ ,$$

$$\vec{P} = K(\sin\theta_1 + \sin\theta_2)\vec{x}_o + K(\cos\theta_2 - \cos\theta_1)\vec{z}_o$$

$$ds = \sec\beta dx, \quad \tan\beta = \xi'(x) \ .$$

For a one dimensional rough surface extending from x=-L to L, Equation (4.13) may be rewritten in the scalar form.

$$E_2 = \frac{ike^{ikR_o}}{4\pi R_o}\int_{-L}^{L} (a\xi - b)e^{iV\ X + iV_z\xi}dx \qquad (4.14)$$

where

$$a = (1-R)\sin\theta_1+(1+R)\sin\theta_2 \quad , \tag{4.15}$$

$$b = (1+R)\cos\theta_2-(1-R)\cos\theta_1 \quad . \tag{4.16}$$

The scattering coefficient ρ is defined as

$$\rho=\frac{E_2}{E_{20}} \quad . \tag{4.17}$$

Where E_{20} is the potential reflected in the direction of specular direction ($\theta_2=\theta_1$) by a smooth plane medium-air interface of the same dimension. In this case

$$V_x = o,\ \xi = \xi' = o,\ R = -1,\ \theta_1 = \theta_2$$

so that

$$E_{20} = \frac{ike^{ikR_o}}{4\pi R_o}\int_{-L}^{L} -bdx = \frac{ike^{ikR_o}}{4\pi R_o}\int_{-L}^{L} -2R\cos\theta_1 dx \ ,$$

or

$$E_{20} = \frac{ike^{ikR_o L\cos\theta_1}}{\pi R_o} \quad . \tag{4.18}$$

Hence, from Equations (4.14), (4.17), and (4.18),

$$\rho = \frac{1}{4L\cos\theta_1}\int_{-L}^{L}(a\xi'-b)e^{iV_xX+iV_z\xi}dx \quad . \tag{4.19}$$

For a smooth surface,

$$\rho = \frac{1}{4L\cos\theta_1}\int_{-L}^{L} (1+R)\cos\theta_2-(1-R)\cos\theta_1 \ e^{iV_xX}dx$$

$$= -\frac{(1+R)\cos\theta_2-(1-R)\cos\theta_1}{2\cos\theta_1}\cdot \mathrm{sinc}V_xL \quad , \tag{4.20}$$

where

$$\mathrm{sinc}\ V_xL = \frac{\sin V_xL}{V_xL} \quad .$$

As a special case, if R=-1, then ρ in Equation (4.20) becomes

$$\rho_o = \text{sinc } V_x L \quad . \tag{4.21}$$

For a rough surface with constant reflection coefficient R, a and b are constant; from Equation (4.19),

$$\rho = \frac{1}{4L\cos\theta_1}\left[-(b+a\frac{V_x}{V_z})\int_{-L}^{L} e^{i\vec{v}\cdot\vec{r}}dx - \frac{i\sigma}{v_z} e^{i\vec{v}\cdot\vec{r}}\Big|_{-L}^{L}\right]$$

$$= -\frac{1}{4L\cos\theta_1}\cdot\frac{2R+2R\cos(\theta_1+\theta_2)}{\cos\theta_1+\cos\theta_2}\int_{-L}^{L} e^{i\vec{v}\cdot\vec{r}}dx - e(L).$$

The second term accounts for the edge effect tends to zero when $L>>\lambda$. Thus, ignoring the edge effect,

$$\rho = \frac{F}{2L}\int_{-L}^{L} e^{i\vec{v}\cdot\vec{r}}dx \quad , \tag{4.22}$$

where

$$F = -R\sec\theta_1 = \frac{1+\cos(\theta_1+\theta_2)}{\cos\theta_1+\cos\theta_2} \quad , \tag{4.23}$$

$$\vec{v}\cdot\vec{r} = \frac{2\pi}{\lambda}[(\sin\theta_1-\sin\theta_2)x-(\cos\theta_1+\cos\theta_2)\xi(x)] \tag{4.24}$$

4.2 Rough surface as random process

The surface height $\xi(x)$ is assumed to be a random variable assuming values z with a probability density w(z), the mean value, denoted by angular bracket <> , is

$$\langle\xi(x)\rangle = 0 \quad , \tag{4.25}$$

and the mean value of the integral for a stationary random surface is

$$\int_{-L}^{L} e^{i\vec{v}\cdot\vec{r}}dx = \int_{-L}^{L} e^{iv_x x}\ e^{iv_z \xi}\ dx$$

$$= e^{iv_z\xi}\int_{-L}^{L} e^{iv_x x}dx$$

$$= \chi(v_z)\int_{-L}^{L} e^{iv_x x}dx \quad . \qquad (4.26)$$

$\chi(v_z) = \int_{-\infty}^{\infty} w(z)e^{iv_z z}dz$ is the characteristic function associated with the distribution w(z). From Equation (4.26) the mean scattering coefficient

$$\langle\rho\rangle = \frac{F}{2\delta}\,\chi(v_z)\,\text{sinc}\ v_x L \quad . \qquad (4.27)$$

The variance of the scattering coefficient $D\{\rho\}$ corresponding to the mean of the normalized scattered power is defined as

$$\langle\rho\rho^*\rangle = \left\langle\left|\frac{E_2}{E_{20}}\right|^2\right\rangle = D\{\rho\} + \langle\rho\rangle\langle\rho^*\rangle \quad . \qquad (4.28)$$

The asterisk * denotes the complex conjugate, and from Equation (4.22),

$$\rho\rho^* = \frac{F^2}{4L^2}\int_{-L}^{L}\int_{-L}^{L} e^{iv_x(x_1-x_2)}\ e^{iv_z(\xi_1-\xi_2)}\ dx_1dx_2$$

Denoting $e^{iv_z(\xi_1-\xi_2)}$ by $\chi_2(v_z-v_z)$, then from Equation (4.28),

$$\rho\rho^* = \frac{F}{4L^2}\int_{-L}^{L}\int_{-L}^{L} \chi_2(v_z,-v_z)\ e^{iv_x(x_1-x_2)}dx_1dx_2$$

where

$$\chi_2(v_z-v_z) = e^{iv(\xi_1-\xi_2)} = \int_{-\infty}^{\infty}\int_{-\infty}^{\infty} w(z_1,z_2)e^{iv_z(\xi_1-\xi_2)}dz_1dz_2$$

and

$$\xi_1 = \xi(x_1) \ , \quad \xi_2=\xi(x_2) \ .$$

$\chi_2(v_z,-v_z)$ is the two-dimensional characteristic function of the distribution $w(z_1, z_2)$. The random rough surface is assumed to have a Gaussian distribution

$$w(z) = \frac{1}{\sqrt{2\pi}\sigma 2} \ e^{-z^2/2\sigma^2} \tag{4.30}$$

and the two-dimensional distribution is

$$w(z_1,z_2,\tau) = \frac{1}{2\pi\sigma^2\sqrt{1-c^2(\tau)}} \cdot \exp\left[-\frac{z_1^2-2c(\tau)z_1z_2+z_2^2}{2\sigma^2(1-c^2(\tau))}\right] \tag{4.31}$$

$\sigma^2 = \langle z^2 \rangle$ is the variance of the rough surface,

$c(\tau)=\frac{\langle z_1z_2\rangle}{\langle z_1^2\rangle}$ is the autocorrelation function of the rough surface,

$\tau=x_1-x_2$ is the separation factor between two points x_1 and x_2.

The autocorrelation function usually assumes the following two forms:

(i). $c(\tau)=e^{-\tau^2/T^2}$ gaussian correlated, (4.32)

(ii). $c(\tau)=e^{-|\tau|/T}$ exponentially correlated, (4.33)

T is called the correlation distance, which is much less than L to assure a random surface.

The one- and two-dimensional characteristic functions are

evaluated as below (Appendix):

$$\chi(v_z) = \int_{-\infty}^{\infty} \frac{1}{\sqrt{2\pi\sigma^2}} e^{-z^2/2\sigma^2} e^{iv_z z}\, dz$$

$$= e^{-\frac{1}{2}\sigma^2 v_z^2}$$

$$= e^{-\frac{1}{2}g} \qquad (4.34)$$

where

$$g = \sigma^2 v_z^2 \zeta \qquad (4.35)$$

$$\chi_2(v_z,-v_z) = \int_{-\infty}^{\infty}\int_{-\infty}^{\infty} w(z_1,z_2\tau) e^{iv_z(z_1-z_2)} dz_1 dz_2$$

$$= \exp -g(1-c(\tau)) \quad . \qquad (4.36)$$

From Equations (4.22), (4.26), (4.28), and (4.29), the variance of ρ is

$$D\{\rho\} = \langle\rho\rho^*\rangle - \langle\rho\rangle\langle\rho^*\rangle$$

$$= \frac{F^2}{4L^2}\int_{-L}^{L}\int_{-L}^{L} e^{iv_x(x_1-x_2)}\ \chi_2(v_z,-v_z) - \chi(v_z)\chi^*(v_z)\ dx_1 dx_2 . \qquad (4.37)$$

Using the relative coordinate τ already defined as

$$\tau = x_1 - x_2 \ , \qquad (4.38)$$

and introducing the center-of-mass coordinate

$$X_o = \frac{1}{2}(x_1+x_2) \qquad (4.39)$$

the equation (4.37) can be rewritten as

$$D\{\rho\} = \frac{F^2}{4L^2}\int_{-L}^{L} dx_o \int_{-2L}^{2L} \left[e^{iv_x\tau}\ \chi_2(\tau) - \chi\chi^*\right] \frac{\partial(x_1,x_2)}{\partial(x_o,\tau)}\, d\tau$$

$$= \frac{F^2}{4L^2} \cdot 2L \cdot \int_{-2L}^{2L} \left[e^{iv_x\tau}\ \chi_z(\tau) - \chi\cdot\chi^*\right] \cdot \det \begin{bmatrix} 1 & -1/2 \\ 1 & +1/2 \end{bmatrix} d\tau$$

$$= \frac{F^2}{2L} \int_{-2L}^{2L} e^{iv_x\tau} \left[\chi_2(\tau) - \chi\chi^*\right] d\tau \ .$$

From Equations (4.34) and (4.36), $D\{\rho\}$ can be expressed in terms of $c(\tau)$ as

$$D\{\rho\}=\frac{F^2}{2L}e^{-g}\int_{-2L}^{2L} e^{iv_x\tau}(e^{gc(\tau)}-1)d\tau \quad . \tag{4.40}$$

Two kinds of correlation functions, Gaussian and exponential, are considered for $g<<1$, and $g>>1$.

(i). Gaussian correlated surface,

(A) If $g\leq 1$, $e^{gc(\tau)}$ can be expanded by a uniformly convergent series.

$$D\{\rho\}=\frac{F^2}{2L}e^{-g}\int_{-2L}^{2L} e^{iv_x\tau}\sum_{m=1}^{\infty}\frac{g^m c^m(\tau)}{m!}d\tau$$

$$=\frac{F^2}{2L}e^{-g}\int_{-\infty}^{\infty} e^{iv_x\tau}\sum_{m=1}^{\infty}\frac{g^m c^m(\tau)}{m!}d\tau, \text{ since } L>>T$$

$$=\frac{\sqrt{\pi}TF^2}{2L}\,e^{-g}\sum_{m=1}^{\infty}\frac{g^m}{m!\sqrt{m}}\,e^{\frac{-v_x^2T^2}{4m}} \quad . \tag{4.41}$$

If $g<<1$,

$$D\{\rho\}=\frac{\sqrt{\pi}TF^2g}{2L}\exp\left[-v_x^2T^2/4\right]; \tag{4.42}$$

$g\simeq 1$

$$\frac{TF^2g}{2L}\,e^{-g}e^{-v_x^2T^2/4}< D\{\rho\} < \frac{\sqrt{\pi}TF^2}{2L} \quad . \tag{4.43}$$

(B) $g>>1$,

$$D\{\rho\} = \frac{F^2}{2L}\int_{-2L}^{2L} e^{iv_x\tau}\left[e^{-g(1-e^{-\tau^2/T^2})}-1\right]d\tau$$

$$= \frac{F^2}{2L}\int_{-2L}^{2L} e^{iv_x\tau}e^{-g(1-e^{-\tau^2/T^2})}d\tau-2F^2e^{-g}\text{sinc}2v_xL$$

$$\simeq \frac{F^2}{2L}\int_{-\infty}^{\infty} e^{iv_x\tau}e^{-g(1-e^{-\tau^2/T^2})}d\tau$$

Because g is much greater than unity, the integrand is neglible if τ/T is not in the close vicinity of zero; the integral is therefore simplified as

$$D\{\rho\}\frac{F^2}{2L} = \int_{-\infty}^{\infty} e^{iv_x\tau} e^{-g\left[1-(1-\tau^2/T^2)\right]}\, d\tau$$

$$= \frac{F^2}{2L}\int_{-\infty}^{\infty} e^{iv_x\tau} e^{-g\tau^2/T^2}\, d\tau$$

$$= \frac{TF^2}{2L}\,\frac{\pi}{g}\,\exp\left[-\frac{v_x^2T^2}{4g}\right] . \qquad (4.44)$$

(ii). Exponentially correlated surface: the same procedure in (i) can be followed.

(A) $g \leq 1$,

$$D\{\rho\}\,\frac{\sqrt{\pi}F^2}{L}\, e^{-g} \sum_{m=1}^{\infty} \frac{g^m}{m!}\,\frac{\sqrt{m}T^2}{m^2+v_x^2T^2} , \qquad (4.45)$$

if $g \ll 1$,

$$D\{\rho\} = \frac{\sqrt{\pi}F^2}{L} \cdot \frac{gT^2}{1+v_x^2T^2} . \qquad (4.46)$$

(B) $g \gg 1$,

$$D\{\rho\} = \frac{F^2}{L} \cdot \frac{gT}{g^2+v_x^2T^2} . \qquad (4.47)$$

4.3 Statistical distribution of the field

The mean scattered field and power is shown in Equation (4.2); the probability distribution of those quantities can be found by looking at the random variable ρ. From Equation (3.22),

$$\rho = \frac{F}{L}\int_{-L}^{L} e^{i\vec{v}\cdot\vec{r}}dx = \frac{F\Delta x}{L}\lim_{n\to\infty}\sum_{j=1}^{n} e^{iv_x x_j + iv_z \xi(x_j)}$$

$$= A\sum_{j=1}^{\infty} e^{i\psi_j}$$

$$= re^{i\psi} \quad . \tag{4.48}$$

$A = \frac{F\Delta x}{L}$ is a constant, and ψ_j is a random quantity. Beckmann has shown that for a very rough random surface ($g>>1, <\rho>\doteq o$) with zero mean $<\rho>=o$, the distribution of the resultant phase ψ is uniform

$$w(\psi) = \frac{1}{2\pi} \quad , \ -\pi<\psi<\pi, \tag{4.49}$$

and the distribution of the amplitude r is Rayleigh distributed

$$w(r) = \frac{2r}{D\{\rho\}}\, e^{-r^2/D\{\rho\}} \quad . \tag{4.50}$$

The variance of $\rho\rho^*$ is found to be

$$D\{\rho\rho^*\} = \int_0^\infty r^4 p(r)dr - D^2\{\rho\}$$

$$\simeq \int_0^\infty \frac{2r^5}{D\{\rho\}} e^{-r^2/D\{\rho\}} dr - D^2\{\rho\}$$

$$= D^2\{\rho\} \tag{4.51}$$

The standard deviation of $\rho\rho^*$

$$\sqrt{D\{\rho\rho^*\}} = D\{\rho\} \tag{4.52}$$

The normalized scattered power $\rho\rho^*$ is found having its mean value and standard deviation equal to $D\{\rho\}$

4.4 The effect of absorption in the medium

The presence of absorption of the space in which the wave

is transmitted has a great influence on the mean scattered powers. The damped wave equation has a general solution

$$E = e^{i\vec{k}\cdot\vec{r}(1-i\alpha/k)-i\omega t} ,$$

which implies a change in the value of V_x and V_z of Equation (4.13).

Let

$$V_x' = V_x - i\frac{\alpha}{K} V_x ,$$

$$V_z' = V_z - i\frac{\alpha}{K} V_z ,$$

$$\chi(v_z') = \frac{1}{\sqrt{2\pi\sigma^2}} \int_{-\infty}^{\infty} e^{-z^2/2\sigma^2} e^{i(v_z - i\frac{\alpha}{k}v_z)z} dz$$

$$= e^{i\sigma^2 v_z^2 \alpha/k} . e^{-\left[\frac{\sigma^2 v_z^2}{2}(1-\frac{\alpha^2}{k^2})\right]}$$

$$= e^{ig2/k} . e^{-\left[\frac{g}{2}(1-\frac{\alpha^2}{k^2})\right]} . \qquad (4.53)$$

Hence,

$$\chi(v_z)\chi^*(v_z) = e^{-g(1-\alpha^2/k^2)} . \qquad (4.54)$$

The two-dimensional characteristic function $\chi_2(v_z', -v_z')$ is

$$\chi_2(v_z', -v_z') = \frac{1}{\sqrt{2\pi\sigma^2}} \int_{-\infty}^{\infty} e^{iv_z(1-i\alpha/k)(1-c)z_2} . e^{\left(-\frac{z_2^2}{2\sigma^2}\right)} dz_2$$

$$\cdot \int_{\infty}^{\infty} \frac{e^{-\frac{(z_1-cz_2)^2}{2\sigma^2(1-c^2)}}}{\sqrt{2\pi\sigma^2(1-c^2)}} e^{iv_z(1-i\alpha/k)(z_1-cz_2)} d(z_1-cz_2)$$

$$= \frac{e^{ig\alpha/k} . e^{-\frac{g}{2}(1-\alpha^2/k^2}}{\sqrt{2\pi\sigma^2}} \int_{-\infty}^{\infty} e^{i(1-c)v_z(1-i\alpha/k)z_2} \cdot e^{-(z_2^2/2\sigma)} dz_2$$

$$= e^{ig\alpha c/k} . e^{-g(1-\alpha^2/k^2)(1-c)} , \qquad (4.55)$$

$$D\{\rho\} = \frac{F^2}{2_L}\int_{-2L}^{2L} e^{iv_x\tau}\ e^{ig\alpha c/k}.\exp\ -g(1-\alpha^2/k^2)(1-c)\ -\exp\left[-g(1-\alpha^2/k^2)\right]d\tau$$

For a very rough surface ($g>>1$), $c(\tau)$ is significant only for very small value of τ/T,

$$D\{\rho\} = \int_{-\infty}^{\infty} e^{iv_x}\ .\exp\ \left[-g(1-\alpha^2/k^2)(1-c)\right]e^{ig\alpha c/k}d\tau\ ,$$

or

$$D\{\rho\} = \frac{F^2}{2_L}\int_{-\infty}^{\infty} e^{iv_x\tau}\ \exp\left[-g(1-\alpha^2/k^2)(1-c)\right]\ d\tau\ . \qquad (4.56)$$

From the analogy between (4.56) and (4.40), the variance of ρ, i. e. $D\{\rho\}$ is

(i). Gaussian correlated surface:

$$D\{\rho\} = \frac{TF^2}{2_L}\cdot\frac{\pi}{g(1-\alpha^2/k^2)}\cdot\exp\left[-\frac{v_x{}^2T^2}{4g(1-\alpha^2/k^2}\right] \qquad (4.57)$$

(ii). Exponentially correlated surface:

$$D\{\rho\} = \frac{F^2}{L}\cdot\frac{g(1-\alpha^2/k^2)}{g^2(1-\alpha^2/k^2)^2+v_x{}^2T^2}\ . \qquad (4.58)$$

Equations (4.17), (4.57), and (4.58) shows that the abosrption will reduce the value of $\langle EE^*\rangle$, and high-frequency wave causes more attenuation than a low-frequency wave.

4.5 Limitations of the general Kirchhoff method applied to acoustic wave scattering

The acoustic wave reflection coefficient is a function of the local angle of incidence, or alternatively, is a function of θ_1, and $\xi(x)$.

$$R = R(\theta) = R(\theta_1 - \arctan'(x) \quad . \qquad (4.12)$$

The approximations of $\langle a\xi' \rangle$ and $\langle b \rangle$ in Equation (4.14), which are always used for varying reflection coefficient case, are much more complicated in the acoustic wave scattering problems. Owing to the elastic property of the medium when θ_1 increases, the generated waves change mode from one to another and the reflection and transmission coefficients change very rapidly. If the rough surface is chosen to be a gently rolling surface ($T>>\sigma$), the probability distributions of the slope $w(\xi')$ are

(i). Gaussian correlated surface:

$$w(\xi') = \frac{T}{\sqrt{4\pi\sigma^2}} \exp\left[-\frac{T^2\xi^2_{12}}{4\sigma^2}\right], \qquad (4.59)$$

(ii). exponentially correlated surface:

$$w(\xi') = \frac{T}{\sqrt{2\pi\sigma^2}} \exp\left[-\frac{T^2\xi^2_{12}}{2\sigma^2}\right]. \qquad (4.60)$$

$w(\xi')$ in Equations (4.59) and (4.60) imply a more dense distribuiton in the neighborhood of zero slope. If θ_1 is also chosen to be small angle, the value of R can be averaged over as

$$R(\theta_1, \xi') \simeq R(\xi' = \langle \xi \rangle) = R(\theta_1), \text{since } \langle \xi' \rangle = 0 \quad . \qquad (4.61)$$

For longitudinal wave incidence with $\theta_1=0$, from Equations (3.17) and (3.16), the reflection and transmission coefficients are defined as

Reflection coefficient

$$R_{12}(\theta_1) = \frac{z_2 - z_1}{z_2 + z_1} \ , \qquad (4.62)$$

Transmission coefficient

$$D_{12}(\theta_1) = \frac{2z_2}{z_2 + z_1} \cdot \frac{\rho_1}{\rho_2} \ , \qquad (4.63)$$

where

$$z_2 = \frac{\rho_2 C_{2\ell}}{\cos\theta_2} \quad , \quad z_1 = \frac{\rho_1 C_{1\ell}}{\cos\theta_1} \quad . \tag{4.64}$$

If the #2 medium is free space or air and the #1 medium is liquid or solid

$$R(\theta_1) = -1 \quad ,$$

$$R(\theta_1) = 0 \quad . \tag{4.65}$$

Under the previous assumptions, a and b in Equation (4.14) are considered to be constant and the general Kirchhoff approximation can be applied to the acoustic wave problems.

5. ACOUSTIC WAVE SCATTERING FROM LAYER

5.1 Layer with rough interface in the back

The evaluation of the scattering field from a very thick layer with roughness in the back is a direct extension of the scattering of a rough surface. Thickness d (Fig. 4) is assumed to be

$$d >> L,$$

so that the smooth boundary of the layer is at the far field of the random rough boundary. The layer to be discussed is a layer without absorption, so that the wave can transmit in it without attenuation. The smooth interface has the following characteristics, at z = d:

$$|E_3| = D_{12} |E_1| \quad , \tag{5.1}$$

$$|E_2| = D_{21} |E_4| \quad , \tag{5.2}$$

where E_1, E_2, E_3, and E_4 are shown in Fig. 4, and D_{12}, D_{21} are the transmission coefficients.

$$D_{12} = \frac{1}{m} \frac{2z_2}{z_2+z_1} \quad ,$$

$$D_{21} = m \frac{2z_1}{z_2+z_1}$$

$$z_2 = \rho_2 c_{2\ell} \quad , \tag{5.3}$$

$$z_1 = \rho_1 c_{1\ell} \quad ,$$

$$m = \frac{\rho_2}{\rho_1} \quad .$$

The rough surface in the back has the same statistical properties as before. Then,

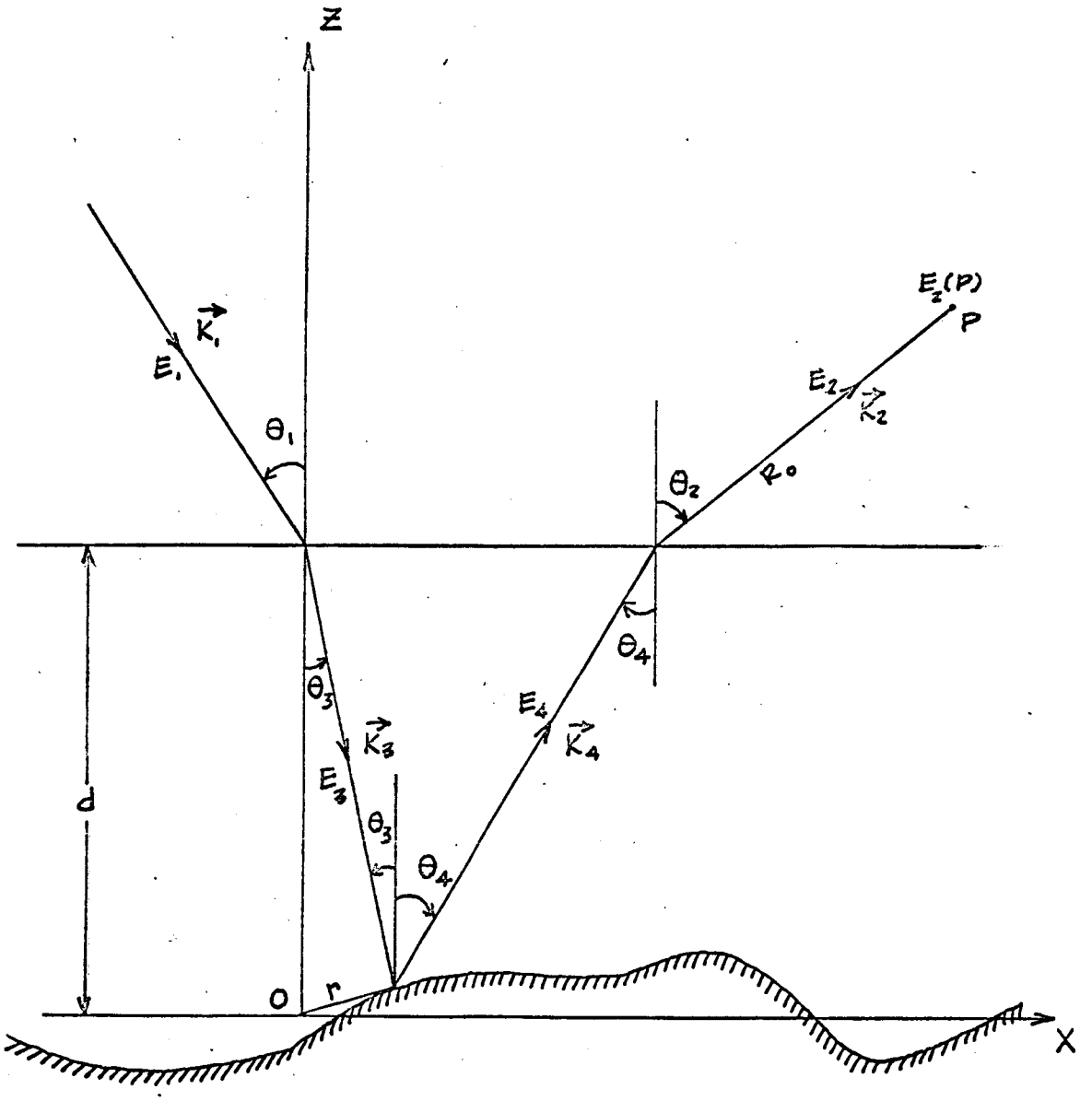

FIG. 4. SCATTERING FROM A LAYER WITH ROUGH SIDE IN BACK

$$E_1 = e^{i\vec{k}_1\cdot\vec{r}+ik_3 d\sec\theta_3} \quad , \tag{5.4}$$

$$E_3 = D_{12}e^{i\vec{k}_3\cdot\vec{r}+ik_3 d\sec\theta_3} \quad , \tag{5.5}$$

The mean scattered field $\langle E_4\rangle$ at a distance R_1 from the origin is

$$\langle E_4\rangle = \frac{ik_3 L e^{i\vec{k}_4\cdot\vec{r}_1+ik_3 d\sec\theta_3}}{\pi R_1} D_{12}\cos\theta_3 e^{-g/2}\cdot\frac{F}{2L}\,\mathrm{sinc}\, v_x L, \tag{5.6}$$

where g and v_x is related to k_3 and

$$\vec{k}_3 = k_3(\sin\theta_3\vec{x}_o - \cos\theta_3\vec{z}_o) \quad ,$$

$$k_3 = |\vec{k}_3| = \frac{2\pi}{\lambda}\cdot\frac{c_{1\rho}}{c_{2\rho}} = n_{12}\frac{2\pi}{\lambda} \quad , \tag{5.7}$$

$n_{12} = \frac{c_{1\rho}}{c_{2\rho}} = \frac{\sin\theta_1}{\sin\theta_3} = \frac{\sin\theta_2}{\sin\theta_4}$ is the Snell's refraction index. The mean scattered power for a very rough surface (g>>1) is

$$\langle E_4E_4^*\rangle = \frac{k_3^2L^2}{\pi^2R_1^2}\cos^2\theta_3\cdot\frac{TF^2}{2L}D_{12}^2\sqrt{\frac{\pi}{g}}\cdot\exp\left[-\frac{v_x^2T^2}{4g}\right] . \tag{5.8}$$

After passing through the smooth interface, the mean scattered field and power, from Equations (5.2), (5.6), and (5.8), are

$$\langle E_2\rangle = \frac{ik_3 L e^{ikR_o+ik_3 d(s\rho c\theta_3+s\rho c\theta_s)}}{\pi(R_o+2d\sec\theta_3)}D_{12}D_{21}\cos\theta_3\cdot\frac{F}{2L}\cdot e^{-g}\mathrm{sinc}v_x L \ , \tag{5.9}$$

$$\langle E_2E_2^*\rangle = \frac{k_3^2L^2D_{12}^2D_{21}^2\cos^2\theta_3}{\pi^2(R_o+2d\sec\theta_3)^2}\cdot\frac{TF^2}{2L}\sqrt{\frac{\pi}{g}}\exp\left[-\frac{v_x^2T^2}{4g}\right] . \tag{5.10}$$

Since

$$E_{20} = \frac{ikLe^{ikR_o\cos\theta_1}}{\pi R_o} \quad ,$$

$$\langle E_{20}E_{20}^{*}\rangle = \frac{k^2L^2\cos^2\theta_1}{\pi^2 R_o^2} \quad ,$$

so that, for $R_o >> 2d\sec\theta_3$,

$$\langle\rho\rangle = \frac{\langle E_2\rangle}{E_{20}} = \eta_{12}D_{12}D_{21}e^{i2k_3d\sec\theta_3}\left(\frac{\cos\theta_3}{\cos\theta_1}\right)\frac{F}{2L}e^{-g/2}\,\mathrm{sinc}v_xL \quad . \tag{5.11}$$

Using Equation (4.37), the variance of ρ can be calculated for different statistical properties of the rough interface.

(i) Gaussian correlated surface:

$$D\{\rho\} = n_{12}^2D_{12}^2D_{21}^2\left[\frac{\cos^2\theta_3}{\cos^2\theta_1}\right]\cdot\frac{TF^2}{2L}\sqrt{\frac{\pi}{g}}\ \exp\left[-\frac{v_x^2T^2}{4g}\right] \quad . \tag{5.12}$$

(ii). Exponentially correlated surface:

$$D\{\rho\} = n_{12}^2D_{12}^2D_{21}^2\left(\frac{\cos^2\theta_3}{\cos^2\theta_1}\right)\cdot\frac{F^2}{L}\cdot\frac{gT}{g^2+v_x^2T^2} \quad . \tag{5.13}$$

For the back-scattering from a layer against air

$$\theta_2 = -\theta_1 \quad , \quad \theta_4 = -\theta_3 \quad , \quad R = -1 \quad ,$$

$$F = -RS\rho c\theta_3\cdot\frac{1+\cos(\theta_3+\theta_4)}{\cos\theta_3+\cos\theta_4} = \sec^2\theta_3 \quad ,$$

$$v_x = k_3(\sin\theta_3-\sin\theta_4) = 2\eta_{12}k\sin\theta_3 = 2k\sin\theta_1 \quad ,$$

$$v_z = -k_3(\sin\theta_3+\cos\theta_4) = 2\eta_{12}k\cos\theta_3 = -2k\sqrt{\eta_{12}^2-\sin^2\theta_1} \quad , \tag{5.14}$$

$$g = v_z^2\sigma^2 = 4k^2\sigma^2(n_{12}^2-\sin^2\theta_1) \quad ,$$

$$n_{12} = \frac{c_{1\ell}}{c_{2\ell}} \quad .$$

The quantities in Equations (5.11), (5.12) and (5.13) show the backscattering from the rough surface in the back of the layer. The backscattered field from the smooth interface in the front of the layer is negligible except for the normal incidence case, which is equivalent to the reflection in the specular direction. If the pulsed signal is used to approximate a monochromatic plane wave, the backscattering from the front surface can be easily rejected by adjusting the gate position in the experimental measurement.

In the actual case, all layers are more or less absorptive. For a layer constructed with a material which has an attenuation factor α, $\langle\rho\rangle$ and $D\{\rho\}$ should be modified as follow:

$$\langle\rho\rangle = n_{12}D_{12}D_{21}e^{i2n_{12}kd\sec\theta_3}\cdot e^{iy2/k_3}\cdot\left(\frac{\cos\theta_3}{\cos\theta_1}\right)^2 x$$

$$\frac{F}{2L}\cdot\exp\left[-2d\alpha\sec\theta_3-\frac{g}{2}\left(1-\frac{\alpha^2}{k_3^2}\right)\right]\operatorname{sinc}v_xL \quad . \qquad (5.15)$$

(i). Gaussian correlated surface:

$$D\{\rho\} = n_{12}^2D_{12}^2D_{21}^2\left(\frac{\cos\theta_3}{\cos\theta_1}\right)^2\cdot\frac{TF^2}{2L}\sqrt{\frac{\pi}{g(1-\alpha^2/k_3^2)}}$$

$$\cdot\exp\left[-4\alpha d\sec\theta_3-\frac{v_x^2T^2}{4g(1-\alpha^2/k_3^2)}\right] \quad ; \qquad (5.16)$$

(ii). Exponentially correlated surface:

$$D\{\rho\} = n_{12}^2 D_{12}^2 D_{21}^2 \frac{\cos\theta_3}{\cos\theta_1} 2\cdot\frac{F^2}{L}\cdot\frac{g(1-\alpha^2/k_3^2)}{g^2(1-\alpha^2/k_3^2)^2+v_x^2T^2}\cdot$$

$$\exp[-4\alpha d\sec\theta_3] \quad . \tag{5.17}$$

The quantity α^2/k_3^2 is usually very small, so that $(1-\alpha^2/k_3^2)\simeq 1$, but $\exp[-4\alpha d\sec\theta_3]$ is very important, it is nearly unity at low frequency, and decreases very fast as frequency increases. For a layer with a very rough interface in the back

$$\langle\rho\rangle \approx 0 \quad . \tag{5.18}$$

It is observed that the wave backscattered from an absorptive layer with rough side in the back, the attenuation by the absorption increases as frequency increases. Aside from the attenuation by the layer, the wave backscattered from the rough side of the layer has the same characteristics as from a rough surface of the same statistical property, except for a changing in magnitude.

5.2 Layer with rough interface in the front

The acoustic wave passes through the rough interface into the layer, and comes back through it after being reflected by the smooth interface. The mean scattered field is negligible if the rough side is very rough, but the mean scattered power, owing to the complicated phase relationship, is difficult to evaluate. A tentative try without experimental support is made here to look at some aspects of the nature of the backscattering from such a layer. If it is proved to be successful, the same

method can be extended to the layer with both sides rough.

As a first step, the field transmitted into the layer after the wave hits the rough front surface is found by considering the field at Q(Fig. 5),

$$E_3(Q) = \frac{1}{4\pi} \iint_S (E\frac{\partial \Psi}{\partial n} - \Psi\frac{\partial E}{\partial n}) dS \quad , \tag{5.19}$$

where

$$\Psi \simeq \frac{e^{ik_3 R_o - i\vec{k}_3 \cdot \vec{r}}}{R_o} \tag{5.20}$$

$$(E)_s = (1+R)E_1 \quad , \tag{5.21}$$

$$\frac{\partial E}{\partial n}_s = i(1-R)E_1 \vec{k}_1 \cdot \vec{r} \quad . \tag{5.22}$$

From the boundary conditions of the acoustic wave reflection, for small incidence angle θ_1 ,

$$k_1(1-R)E_1 = k_3 D E_1 \quad ,$$

$$\rho_1(1+R)E_1 = \rho_2 D E_1 \quad ,$$

$$(1+R) = \frac{\rho_2}{\rho_1} D = mD \tag{5.23}$$

$$(1-R) = \frac{k_3}{k_1} D = \frac{c_{1\rho}}{c_{2\rho}} D = \eta D \tag{5.24}$$

Substituting Equations (5.23), (5.24) into (5.21) and (5.22)

$$(E)_s = mDE_1 \quad , \tag{5.25}$$

$$\left(\frac{\partial E}{\partial n}\right)_s = i\eta D E_1 \vec{k}_1 \cdot \vec{r} \quad . \tag{5.26}$$

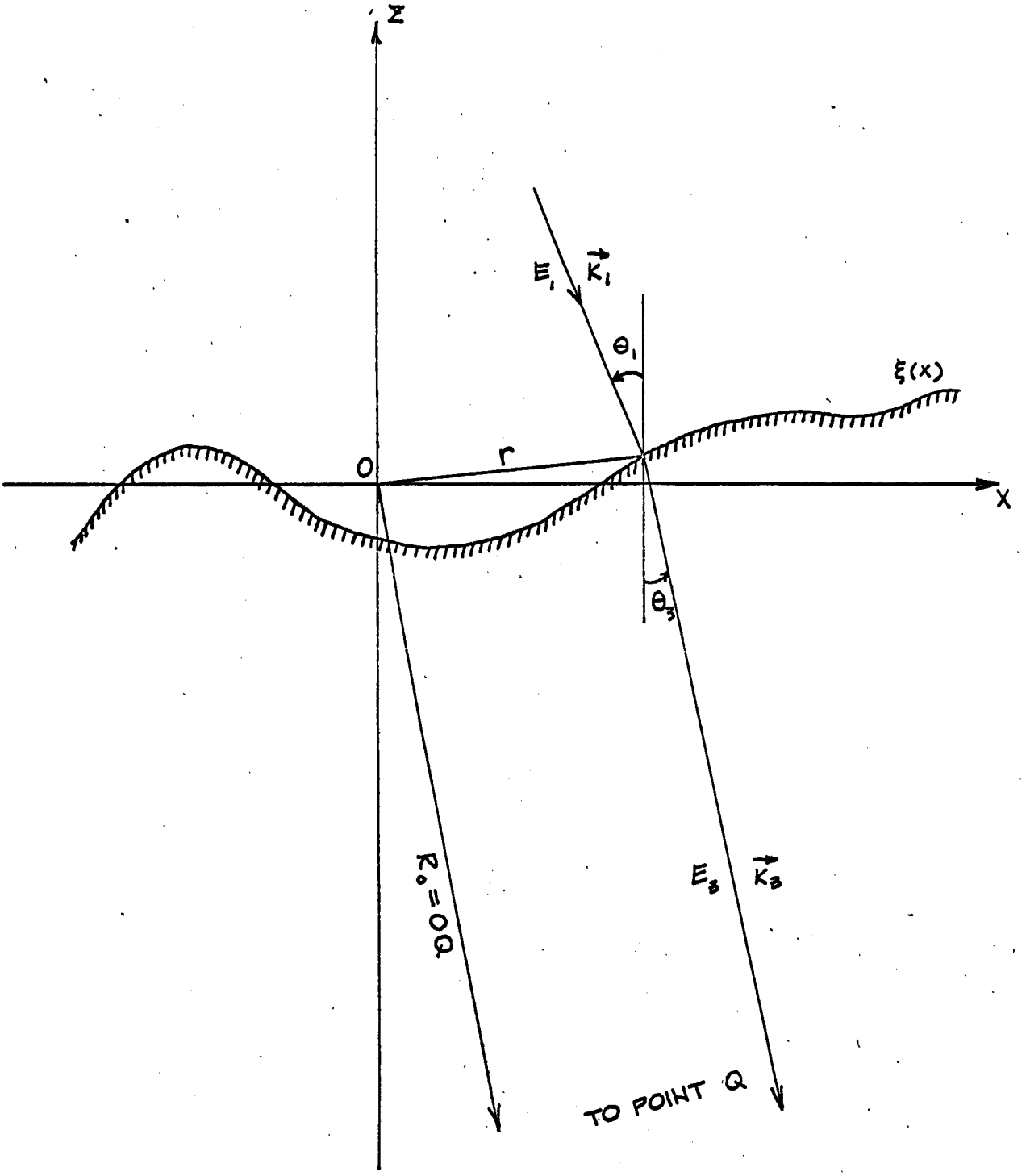

FIG. 5. TRANSMISSION THROUGH A ROUGH INTERFACE

Substituting Equations (5.10), (5.25), (5.26) into (5.19),

$$E_3(Q) = \frac{1}{4\pi}\iint_S [mDE_1(-\psi\vec{k}\cdot\vec{n}) - \psi(inDE_1\vec{k}_1\cdot\vec{n})]ds \quad ,$$

where

$$\vec{n} = -\sin\beta\vec{x}_o + \cos\beta\vec{z}_o \quad ,$$

$$\vec{r} = x\vec{x}_o + \xi(x)\vec{z}_o \quad ,$$

$$\vec{k}_1 = k(\sin\theta_1\vec{x}_o - \cos\theta_1\vec{z}_1) \quad ,$$

$$\vec{k}_3 = nk(\sin\theta_3\vec{x}_o - \cos\theta_3\vec{z}_o) \quad ,$$

$$\vec{w} = \vec{k}_1 - \vec{k}_3$$

$$= k(\sin\theta_1 - n\sin\theta_3)\vec{x}_o - k(\cos\theta_1 - n\cos\theta_3)\vec{z}_o$$

$$= w_x\vec{x}_o + w_z\vec{z}_o$$

$$ds = \sec\beta dx \quad , \qquad \tan\beta = \xi'(x) \quad .$$

so that,

$$E_3(Q) = -\frac{inke^{ik_3R_o}}{4\pi R_o}\int_{-L}^{L}(a\xi'-b)e^{i\vec{w}\cdot\vec{r}}dx \quad , \tag{5.27}$$

where

$$a = D(\sin\theta_1 + m\sin\theta_3) \quad , \tag{5.28}$$

$$b = -D(\cos\theta_1 + m\cos\theta_3) \quad .$$

For smooth interface, $\xi = \xi' = 0$,

$$E_3(Q) = \frac{inke^{inkR_o}}{4\pi R_o} \int_{-L}^{L} be^{iw_x x} dx \quad ,$$

or

$$E_3(Q) = - \frac{inke^{inkR_o}L}{2\pi R_o} D(\cos\theta_1 + m \cos\theta_3) \operatorname{sinc} w_x L \quad . \quad (5.30)$$

For the direction $\theta_3 = \arcsin\left(\frac{1}{n}\sin\theta_1\right)$,

$$E_3(Q) = - \frac{inke^{inkR_o}L}{2\pi R_o} D\left(\cos\theta_1 + m\sqrt{1 - \frac{1}{n^2}\sin^2\theta_1}\right) \quad . \quad (5.31)$$

$$E_3(Q) = 0 \quad , \quad \text{otherwise.}$$

For a rough interface,

$$E_3(Q) = - \frac{inke^{inkR_o}}{4\pi R_o} \left[-\left(b + a\frac{w_x}{w_z}\right) \int_{-L}^{L} e^{i\vec{w}\cdot\vec{r}} dx\right]$$

$$= - \frac{inke^{inkR_o}}{4\pi R_o} D \cdot \frac{1 - mn + (m-n)\cos(\theta_3 - \theta_1)}{\cos\theta_1 - n\cos\theta_3} \cdot \int_{-L}^{L} e^{i\vec{w}\cdot\vec{r}} dx \quad ,$$

or

$$E_3(Q) = \frac{e^{inkR_o}}{R_o} \cdot \frac{G}{2L} \int_{-L}^{L} e^{i\vec{w}\cdot\vec{r}} dx \quad (5.32)$$

where,

$$G = - \frac{inkD}{2\pi} \cdot \frac{1 - mn + (m-n)\cos(\theta_2 - \theta_1)}{\cos\theta_1 - n\cos\theta_3} \quad ,$$

$$\vec{w}\cdot\vec{r} = K\left[(\sin\theta_1 - n\sin\theta_3)x - (\cos\theta_1 - n\cos\theta_3)\xi\right] \quad . \quad (5.33)$$

Equations (5.32) and (5.33) are analogues of the equations for scattering from a rough surface. The mean field and mean scattered power can be written down in similar form.

$$\langle E_3 \rangle = \frac{e^{ikR_o}}{R_o} \cdot \frac{G}{2L} e^{-\frac{h}{2}} \operatorname{sinc} w_x L \quad . \tag{5.34}$$

If it is a very rough interface ($h = w_z^2 \sigma^2 >> 1$) ,

$$\langle E_3 \rangle \approx 0$$

and,

(i) Gaussian correlated interface:

$$\langle E_3 E_3^* \rangle = \frac{TG^2}{2LR_o^2} \sqrt{\frac{\pi}{h}} \cdot \exp\left[-\frac{w_x^2 T^2}{4h}\right] \quad ; \tag{5.35}$$

(ii) Exponentially correlated interface:

$$\langle E_3 E_3^* \rangle = \frac{G^2}{LR_o^2} \cdot \frac{hT}{h^2 + w_x^2 T^2} \quad . \tag{5.36}$$

Equations (5.32) to (5.36), which are derived under the assumption that the incidence angle to be very small, show the properties of the transmission through a very rough interface. The next step is to find the effect of the layer's second interface, thus obtaining the overall effect of the layer with rough side in front. This layer is essentially the same as the previous one in section 5.1, except it has been turned over with rough side facing the incident wave (Fig. 6). The field E_3 strikes the lower plane interface at $z = 0$ and produces a reflected field E_4 in the specular direction only (see Fig. 6). If R_1 is defined as the distance from the point 0_1 to the point of observation Q

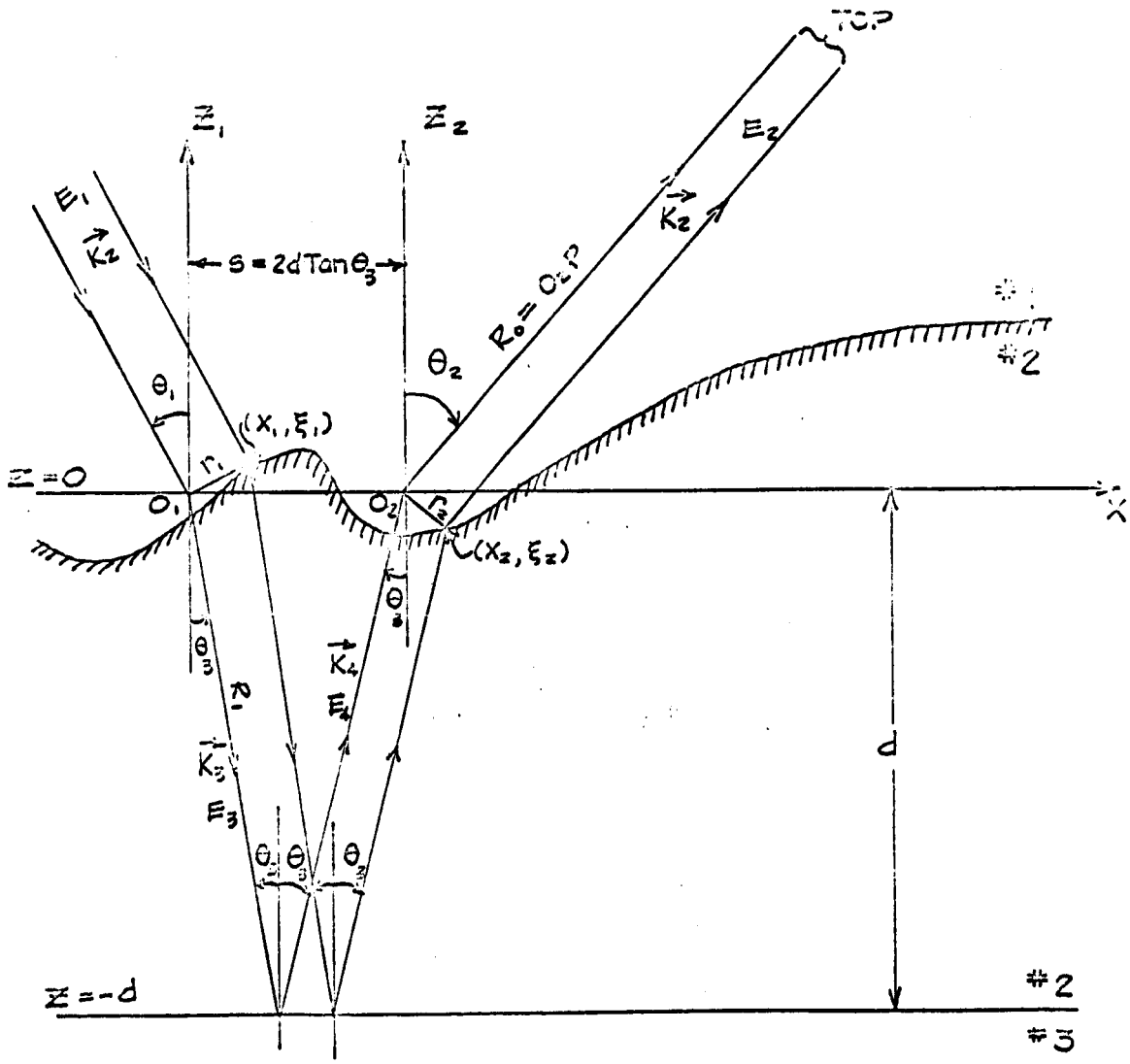

FIG.6. SCATTERING FROM A LAYER WITH ROUGH SIDE IN FRONT

below the rough interface, then

$$E_3 = \frac{e^{inkR_1}}{R_1} \cdot \frac{G_1}{2L} \int_{-L}^{L} e^{i\vec{w}_1 \cdot \vec{r}_1} dx_1 \quad ,$$

and the reflected field E_4 is related to E_3 by the following boundary condition:

$$(E_4)_{z=-d} = (R_{23} E_3)_{z=-d} \quad .$$

Under this boundary condition, the field E_4 incident on the rough surface from below is

$$(E_4)_{z=\xi(x)} = \left(\frac{e^{i2k_3 d \sec\theta_3}}{2(d-\xi)\sec\theta_3} \cdot R_{23} \cdot \frac{G}{2L} \int_{-L}^{L} e^{i\vec{w}_1 \cdot \vec{r}_1} dx_1 \right) \cdot e^{i\vec{k}_4 \cdot \vec{r}_2} \quad (5.37)$$

The transmitted field $E_2(P)\theta_3$ caused by the incidence of $(E_4)_{z=\xi}$ can be derived from Equation (5.32), here the subscript θ_3 denotes that the field $E_2(P)_{\theta_3}$ is contributed only by the component of E_4 in the direction of $\vec{k}_4$. Then,

$$E_2(P)\theta_3 = \frac{e^{i2k_3 d \sec\theta_3} \cdot e^{ikR_o}}{2R_o(d-\xi)\sec\theta_3} \cdot R_{23} \cdot \frac{G_1 G_2}{4L^2} \int_{-L}^{L}\int_{-L}^{L} e^{i(\vec{w}_1\vec{r}_1 + \vec{w}_2 \cdot \vec{r}_2)} dx_1 dx_2 \quad (5.38)$$

where

$$G_1 = - \frac{inkLD_{12}}{2\pi} \cdot \frac{1-mn+(m-n)\cos(\theta_3-\theta_1)}{\cos\theta_1 - n\cos\theta_3} \quad ,$$

$$G_2 = - \frac{iKLD_{21}}{2\pi} \cdot \frac{1-\frac{1}{mn}+(\frac{1}{m}-\frac{1}{n})\cos(\theta_2-\theta_3)}{\cos\theta_3 - \frac{1}{n}\cos\theta_2} \quad ,$$

$$\vec{w}_1 = \vec{k}_1 - \vec{k}_3$$

$$= k(\sin\theta_1 - n\sin\theta_3)x_o - k(\cos\theta_1 - n\cos\theta_3)z_o$$

$$= W_{x1}\vec{X}_o + W_{z1}\vec{Z}_o \quad , \tag{5.39}$$

$$\vec{w}_2 = \vec{k}_4 - \vec{k}_2$$

$$= k(n\sin\theta_3 - \sin\theta_1)\vec{X}_o + k(n\cos\theta_3 - \cos\theta_1)\vec{Z}_o$$

$$W_{x2}\vec{X}_o + W_{z2}\vec{Z}_o \quad ,$$

$$\vec{r}_1 = x_1\vec{x}_o + \xi(x_1)\vec{Z}_o \quad ,$$

$$\vec{r}_2 = x_2\vec{x}_o + \xi(s+x_2)\vec{Z}_o \quad .$$

It should be noted here that $\vec{r}_1$ and $\vec{r}_2$ are refered to origins 0_1 and 0_2, respectively. And more-over, since the maximum value of $\xi(X)$ is much less then the thickness of the layer, so that,

$$E_2(P)_{\theta_3} = \frac{e^{i2k_3 d\sec\theta_3}\cdot e^{ikR_o}}{2R_o d\sec\theta_3}\cdot R_{23}\cdot\frac{G_1G_2}{4L^2}\int_{-L}^{L}\int_{-L}^{L} e^{i(\vec{w}_1\cdot\vec{r}_1+\vec{w}_2\cdot\vec{r}_2)}dx_1dx_2 \tag{5.40}$$

In the backscattering direction, $\theta_2 = -\theta_1$, then

$$G_1 = -\frac{inkLD_{12}}{2\pi}\cdot\frac{1-mn+(m-n)\cos(\theta_3-\theta_1)}{\cos\theta_1-n\cos\theta_3} \quad ,$$

$$G_2 = -\frac{ikLD_{21}}{2\pi}\cdot\frac{1-\frac{1}{mn}+(\frac{1}{m}-\frac{1}{n})\cos(\theta_3+\theta_1)}{\cos\theta_1-n\cos\theta_3} \quad , \tag{5.41}$$

$$\vec{W}_1 = K(\sin\theta_1-n\sin\theta_3)\vec{x}_o - k(\cos\theta_1-n\cos\theta_3)\vec{z}_o \quad ,$$

$$\vec{W}_2 = k(\sin\theta_1+n\sin\theta_3)\vec{x}_o - k(\cos\theta_1-n\cos\theta_3)\vec{z}_o \quad .$$

From Equations (5.40) and (5.41), the mean value of $E_2(P)\theta_3$ can be found,

$$\langle E_2(P)\theta_3\rangle = \frac{e^{i2kd\sec\theta_3}\cdot e^{ikR_o}}{2R_o d\sec\theta_3}\cdot R_{23}\cdot\frac{G_1G_2}{4L^2}\int_{-\infty}^{\infty}\int_{-\infty}^{\infty} W(Z_1,Z_2,s)\,dz_1dz_2\cdot$$

$$\int_{-L}^{L}\int_{-L}^{L} e^{i(\vec{w}_1\cdot\vec{r}_1+\vec{w}_2\vec{w}_2)}\,dx_1dx_2 \quad , \quad (5.42$$

where s in Equation (5.42) is the separation factor between ξ_1 and ξ_2 ,

$$s = (2d+\xi_1+\xi_2)\tan\theta_3 \quad .$$

Since $|\xi_{max}| << d$,

$$s \approx 2d\tan\theta_3 \quad . \qquad (5.43$$

Hence, from Equation (5.42).

$$\langle E_2(P)\theta_3\rangle = A\cdot\exp[-h(1+c(s)]\cdot\mathrm{sinc}[kL(\sin\theta_1-n\sin\theta_3)]$$

$$\cdot\mathrm{sinc}[kL(\sin\theta_1+n\sin\theta_3)] \qquad (5.44)$$

where

$$h = W_z^2\sigma^2$$

$$W_z = -K(\cos\theta_1-n\cos\theta_3) \quad . \qquad (5.45)$$

$$A = \frac{e^{ik_3d\sec\theta_3}\cdot e^{ikR_o}}{2dR_o\sec\theta_3}\cdot R_{23}\cdot\frac{G_1G_2}{4L^2}$$

From Equation (5.44), it is seen that if the front interface is very rough ($h >> 1$),

$$\langle E_2(P)\theta_3\rangle \approx 0$$

and,

$$\langle E_2(P)\rangle = \int_{-\pi/2}^{\pi/2} \langle E_2(P)\theta_3\rangle d\theta_3 = 0 \quad . \tag{5.46}$$

The evaluation of $\langle E_2E_2^*\rangle$ is very much involved, approximations have to be used throughout the derivation. From equation (5.40),

$$(E_2E_2^*)_{\theta_3} = AA^* \int_{-L}^{L}\int_{-L}^{L}\int_{-L}^{L}\int_{-L}^{L} e^{i\vec{w}_1\cdot(\vec{r}_1\cdot\vec{r}_1)+i\vec{w}_2\cdot(\vec{r}_2-\vec{r}_2)} dx_1 dx_2 dx_1' dx_2' \tag{5.47}$$

where the subscripts 1 and 2 are referred to the origions 0_1 and 0_2, respectively (see Fig. 6).

The mean value of $(E_2E_2^*)\theta_3$ over the rough interface is

$$\langle (E_2E_2^*)\theta_3\rangle = AA^* \int_{-L}^{L}\int_{-L}^{L}\int_{-L}^{L}\int_{-L}^{L} \langle e^{iWz(\xi_1-\xi_1')+iW_z(\xi_1-\xi_2')}\rangle$$

$$\cdot e^{iw_{x1}(x_1-x_1')+iW_{x2}(x_2-x_2')} dx_1 dx_2 dx_1' dx_2' \tag{5.48}$$

and from Mood (Mood 1963), the 4th order characteristic function associated with W_z is

$$\chi_4(s,\tau) \equiv \langle e^{iW_z(\xi_1-\xi_1')+iW_z(\xi_2-\xi_2')} \rangle$$

$$= \int_{-\infty}^{\infty}\int_{-\infty}^{\infty}\int_{-\infty}^{\infty}\int_{-\infty}^{\infty} W(z_1,z_2,z_1',z_2',\tau,s)\, e^{iW_z(\xi_1-\xi_1')+iW_z(\xi_2-\xi_2')} \, dz_1 dz_2 dz_1' dz_2'$$

$$= \exp\Big[-\frac{h}{2}(2+2c(s)-2c(\tau_1)-c(s+\tau_1)-c(s-\tau_1) - \frac{h}{2}(2+2c(s)-2c(\tau_2)-c(s+\tau_2)-c(s-\tau_2)\Big] \quad , \qquad (5.49)$$

where

$$\tau_1 = x_1 - x_1' \quad , \text{ and } \tau_2 = x_2 - x_2' \quad . \qquad (5.50)$$

For a Gaussian correlated random surface,

$$c(\tau) = e^{-\tau^2/T^2} \quad ,$$

and as seen from Equation (5.49), the 4th-order characteristic function $\chi_4(s,\tau_1,\tau_2)$ is equal to zero except when

$$s << T, \ \tau_1 << T, \text{ and } \tau_2 << T \quad . \qquad (5.51)$$

In the case shown in Equation (5.51),

$$\chi(s,\tau_1,\tau_2) \approx e^{-h\left[2(\tau_1^2+\tau_2^2)/T^2\right]} . \qquad (5.52)$$

Introducing new coordinates,

$$y_1 = \frac{1}{2}(x_1+x_1') \text{, and } y_2 = \frac{1}{2}(x_2+x_2') \text{,}$$

and using Equation (5.52) for a very rough layer, Equation (5.48) becomes

$$(E_2E_2^*)\theta_3 = AA^* \cdot \int_{-L}^{L}\int_{-L}^{L}\int_{-L}^{L}\int_{-L}^{L} e^{-2h\left(\frac{\tau_1^2}{T^2}+\frac{\tau_2^2}{T^2}\right)} \cdot e^{iW_{x1}\tau+iW_{x2}\tau} d\tau_1 d\tau_2 dy_1 dy_2$$

$$= 4L^2 AA^* \cdot \sqrt{\frac{\pi T^2}{2h}} \cdot \exp\left[-\frac{W_{x_1}^2 T^2}{8h}\right] \cdot \sqrt{\frac{\pi T^2}{2h}} \cdot \exp\left[-\frac{W_{x_2}^2 T^2}{8h}\right],$$

or

$$\langle (E_2 E_2^*)_{\theta_3} \rangle = 2L^2 AA^* \cdot \frac{\pi T^2}{h} \cdot \exp\left[-\frac{W_{x_1}^2 + W_{x_2}^2}{8h} T^2 \right] \quad , \tag{5.53}$$

where

$$h = k^2 \sigma^2 (\cos\theta_1 - n\cos\theta_3)^2 \quad ,$$

$$W_{x_1}^2 + W_{x_2}^2 = 2K^2 (\sin^2\theta_1 + n^2 \sin^2\theta_3) \, . \tag{5.54}$$

Substituting Equation (5.54) into Equation (5.53),

$$\langle (E_2 E_2^*) \theta_3 \rangle = \frac{2\pi T^2 L^2 AA^*}{K^2 \sigma^2 (\cos\theta_1 - n\cos\theta_3)^2} \cdot \exp\left[-T \, (\sin^2\theta_1 + n^2 \sin^2\theta_3) / 4\sigma^2 (\cos\theta_1 - n\cos\theta_3)^2 \right] \tag{5.55}$$

In Equation (5.55), $\langle (E_2 E_2^*) \theta_3 \rangle$ is significant only when θ_1 and θ_3 are very small angles, i. e.,

$$\sin\theta_1 \simeq \theta_1 \quad , \quad \cos\theta_1 \simeq 1 \quad .$$

$$\sin\theta_3 \simeq \theta_3 \quad , \quad \cos\theta_3 \simeq 1 \quad . \tag{5.56}$$

Then, the limit in the integration for obtaining $\langle E_2 E_2^* \rangle$ can be extended to infinity, so that

$$\langle E_2 E_2^* \rangle = \int_{-\pi/2}^{\pi/2} \langle (E_2 E_2^*) \theta_3 \rangle d\theta_3$$

$$\simeq \int_{-\infty}^{\infty} 2L^2 AA^* \cdot \frac{\pi T^2}{K^2 \sigma^2 (1-n)^2} \cdot \exp\left[-T^2 (\theta_1^2 + \theta_3^2) / 4\sigma^2 (1-n)^2 \right] d\theta_3$$

where

$$AA^* = \frac{R_{23}^2}{4d^2 R_o^2 \cdot 16L^4} \cdot \frac{n^2 K^4 L^4 D_{12}^2 D_{21}^2}{16\pi^4} \cdot \frac{\left(|-mn+(m-n)\right)^2 \cdot \left(1 - \frac{1}{m} + (\frac{1}{m} - \frac{1}{n})\right)^2}{(1-n)^4}$$

Rewriting Equation (5.55),

$$\langle E_2 E_2^* \rangle = \frac{R_{23}^2 D_{12}^2 D_{21}^2 L^2 (1+m)^4}{256\pi^{5/2} d^2 R_o^2 m^2 |1-n|} \cdot k^2 \cdot \frac{T}{\sigma} \exp\left[-\theta_1^2 T^2 / 4\sigma^2 (1-n)^2\right] \quad (5.57)$$

Since $E_{20} E_{20}^* \simeq \frac{K^2 L^2}{\pi^2 R_o^2}$, and $\langle E_2 \rangle \simeq o$, the variance of the scattering coefficient ρ becomes

$$D\{\rho\} = \frac{\langle E_2 E_2^* \rangle}{E_{20} E_{20}^*}$$

$$= \frac{R_{23} D_{12} D_{21} (1+m^4)}{256\ \pi m^2 |1-n|} \times \frac{T}{\sigma d^2} \cdot \exp -\theta_1^2 T^2 / 4\sigma^2 (1-n)^2 \quad . \quad (5.58)$$

From Equations (5.46), (5.55) and (5.58), it is seen that the backscatter from a layer with rough side in front is much smaller than that from a layer with rough side in back. Moreover, the parameters of the media has more influence on the backscattered power as compared with the previous one in Section 5.1, and as the incidence angle θ_1 increases, the backscattered power drop off very rapidly.

5.3 Discussion of the derivation

(A) Rough side in back: The fields E_3 and E_4 in the layer have been assumed to be caused by a plane wave and the amplitudes are independent of the thickness "d" of the layer. If the thickness d is much larger then the illuminated length 2L, the amplitudes of E_3 and E_4 will depend on the value of d. From Equation (5.3), introducing the dispersion caused by the thickness of the layer, the value of E_3 given by Equation (5.5) will be changed to

$$E_3 = - \frac{i n_{12} k e^{i\vec{k_3} \cdot \vec{r_1} + ik_3 d \sec\theta_3}}{2\pi R_1} L D_{12} (\cos\theta_1 + m\cos\theta_3) . \quad (5.5a)$$

A similar modification should be made on E_4 and E_2 also. The results of these changes in E_2, E_3, and E_4 will modify $D\{\rho\}$ of Equations (5-12) and (5-13) to the form

$$D\{\rho\}=\frac{n_{12}^6 D_{12}^2 D_{21}^2}{32\pi^4 m^2}\ \frac{\cos^2\theta_3(\cos\theta_1+m\cos\theta_3)^4}{\cos^2\theta_1}\cdot\frac{k^4L^3TF^2}{d^4}\sqrt{\frac{\pi}{g}}\cdot\exp-\frac{V_x^2T^2}{4g}\ ; \tag{5.12a}$$

(ii) exponentially correlated surface:

$$D\{\rho\}=\frac{n_{12}^6 D_{12}^6 D_{21}^2}{16\pi^4 m^2}\ \frac{\cos^2\theta_3(\cos\theta_1+m\cos\theta_3)^4}{\cos^2\theta_1}\cdot\frac{k^4L^3F^2}{d^4}\cdot\frac{gT}{g^2+V_x^2T^2}\ . \tag{5.13a}$$

(B) Rough side in front: Under the same condition, $D\{\rho\}$ in Equation (5.58) should also be modified to the form

$$D\{\rho\}=\frac{n^2K^2R_{23}^2D_{12}^2D_{21}^2(1+m^4)}{256\pi^3m^2|1-n|}\cdot\frac{TL^2}{\sigma d^4}\cdot\exp\left[-\theta_1^2T^2/4\sigma^2(1-n)^2\right]. \tag{5.58a}$$

$D\{\rho\}$ in Equations (5.12a), (5.13a), and (5.58a) are derived under the condition that the layer is very thick. However, in most cases, d is not so much larger than the illuminated length, and the Equations (5.12), (5.13), and (5.58) give us a good estimate on the value of $D\{\rho\}$.

6. EXPERIMENTAL WORK

6.1 Experimental set-up and procedure

The experimental measurement of the variance of the scattering coefficient has been done in the Underwater Acoustic Laboratory, Electrical Engineering Department, Kansas State University. Details of the equipment can be found in the report by Toliver (Toliver 1965). The block diagram of the experimental set-up is shown in Fig. 7.

In the experiment, pulsed signals generated by the pulsed oscillator are sent out and collected by one pair of transducers in the water tank. For each single pulse sent out, the received signal will contain a train of pulses. A gating circuit, which is synchronized by the delayed trigger output from the pulsed oscillator, is used to select the portion of the pulse train for feeding into the detector and boxcar circuit. The boxcar circuit has the function of converting the discrete pulse into an analog signal so that it can be recorded by the graphic level recorder.

The distance S from the transducers to the front side of the target is determined by

$$S = D\cos\theta_1 \tag{6.1}$$

where $\theta_1 = 0^\circ$, 5°, and 10°, and D is the distance travelled by the radiated signal before it hits the target. It is desired to have D as large as possible so that the illuminated area will be much larger than the correlation distance of the random interface. The choice of 32 inches is made to give an average

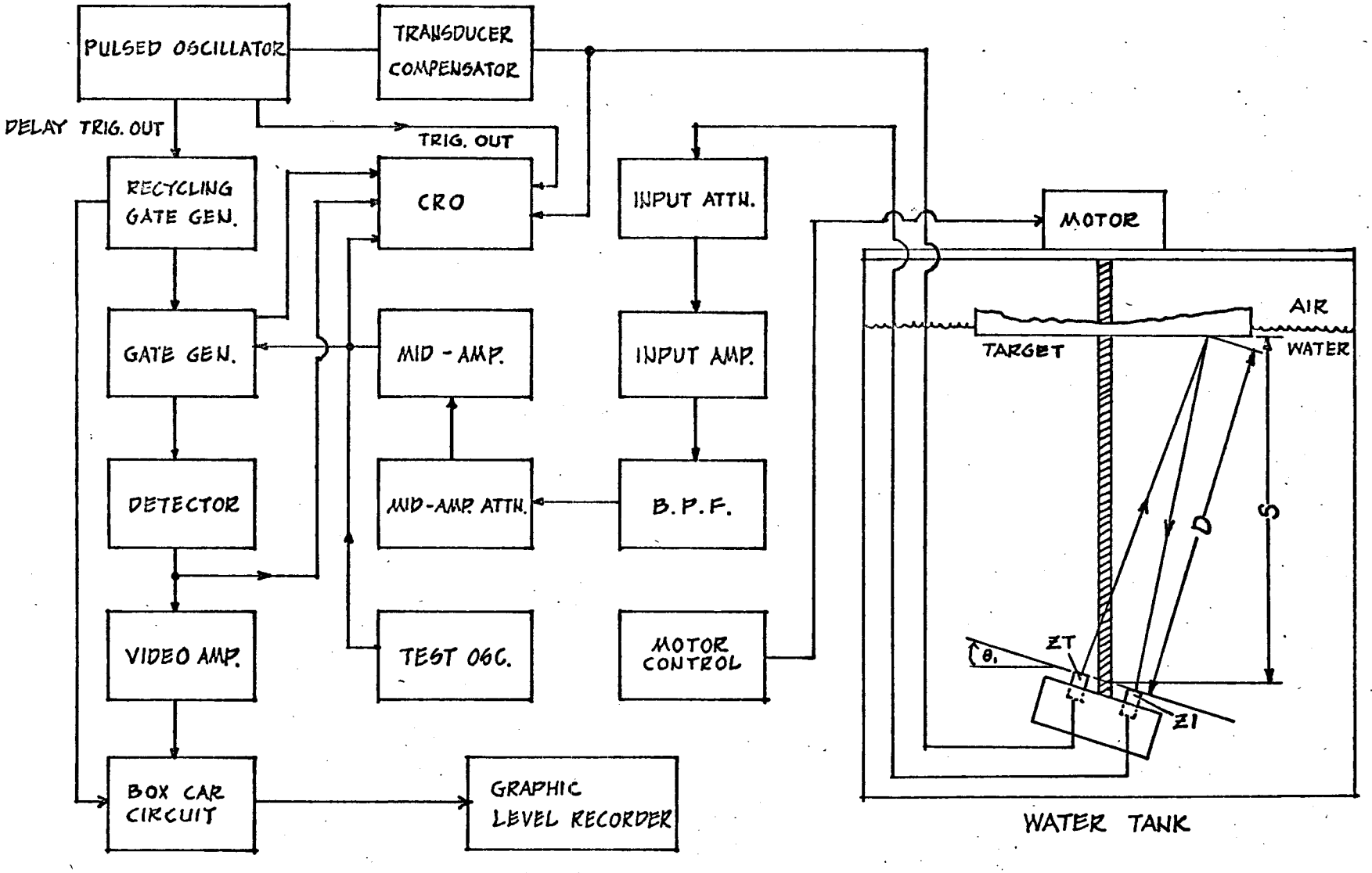

FIG. 7 EXPERIMENTAL SET-UP BLOCK DIAGRAM

value of L = 0.75 inches for different pairs of transducers. The pulse recurrence frequency, PRF, is also determined by D. It is selected to be the largest value without causing any overlapping of the first few returns with the following pulse sent out from the transmitter. And the pulse length, which should be as larger as possible to simulate a monochromatic wave, is limited by the thickness of the layer. The pulse length must be less than the time that is necessary for the wave to make a round trip in the layer. A safety choice of PRF and pulse length for the model target constructed and the distance D specified is as follows:

pulse length = 20 μsec,

PRF = 250 pps.

The operating frequencies are chosen to be

0.72, 1.0, 1.28, 1.6, 1.9, 2.25, 3.0, and 3.5 mc.

Before the measurements of $D\{\rho\}$ start, the folliwng procedures are conducted at $\theta_1 = 0^\circ$, S = D = 32 inches, f = 1 mc.

(a) The target suspension is carefully checked by the returned pulse position on CRO to make sure that D is equal to 32 inches for all possible positions of transducers.

(b) Transducers focusing is done by adjusting the mounting of transducers for maximum return from a smooth plane target 32 inches apart.

After checking on the mounting of target and transducers, measurements proceed as follows:

(c) Setting the operating frequency with the help of test oscillator and CRO.

(d) The pulse length and PRF is set at pulse length = 20μsec. PRF = 250 pps.

(e) The RF output level and the transducer compensator is adjusted to yield the best possible undistorted pulse.

Procedures (c), (d), and (e) are conducted iteratively to fit all the figures required.

(f) Measurement $|E_{20}|$: the water-air interface is used as target, because it acts as perfect reflector; and D = 32 inches, $\theta_1 = 0^o$ are carefully checked. Then the magnitude recorded by the recorder gives

$$M_1 = K_1 AB|E_{20}| \tag{6.2}$$

where A is the magnitude of the output pulse, B is the gain of the transducers, and K_1 is the overall gain of receiver and recorder.

(g) Varying θ_1 to the desired angle (0^o, 5^o, 10^o) and setting S according to the relation shown in Equation (6.1), then $|E_2|$, which is a function of the horizontal position of the transducers, is measured by scanning the transducers through the target. The gate is adjusted in the way that only the return from the back side of the layer is detected and recorded. The sample magnitude of a point on the recording sheet gives

$$M_2 = K_2 AB\ |E_2|\ , \tag{6.3}$$

where K_2 is the overall gain in this measurement. The ratio of K_2 to K_1 can be read from the settings.

Since $\langle\rho\rangle \approx 0$, so that the variance of the scattering coefficient is

$$D\{\rho\} = \langle |\rho|^2 \rangle = \left\langle \frac{|E_2|^2}{E_{20}^2} \right\rangle = \left\langle \frac{M_2^2}{M_1^2} \right\rangle \cdot \left(\frac{K_1}{K_2}\right)^2 ,$$

or

$$D\{\rho\} = \frac{\langle M_2^2 \rangle}{M_1^2} \cdot 10 \left(\frac{k_{db}}{10}\right),$$

where $K_{db} = (K_2/K_1)$ in db is the ratio of the overall receiver gain between the measurement of $|E_2|$ and $|E_{20}|$. Attention must be paid not to overdrive any stage in the steps (f) and (g). K_2 is adjusted to give the maximum possible recording without causing saturation in any one of the amplifiers and in the recording devices.

6.2 Description of layer target

The target is a block of plexiglas with a one-dimensional roughness on one side. (Fig. 8). The length of the plexiglas is limited by the dimension of the water tank; the width is equal to 6 inches, which is much greater then the illuminated area of any pairs of transducers; and the thickness, which should be as thick as possible, is limtied to 2 inches by the material available at the time of construction. The profile of the rough surface on the layer is desired to have a Gaussian probability distribution in height with standard deviation $\sigma = 0.05$ inches, and to have a gaussian autocorrelation with respect to the horizontal position, where the correlation distance is $T = 0.15$ inches. The profile is calculated by trial and error with the help of an IBM 1620 computer. It is noted that the heights between -3σ and $+3\sigma$ were considered in the calculation, and the sample heights obtained from the truncated normal distribution are so arranged that there is no sudden or periodical variations.

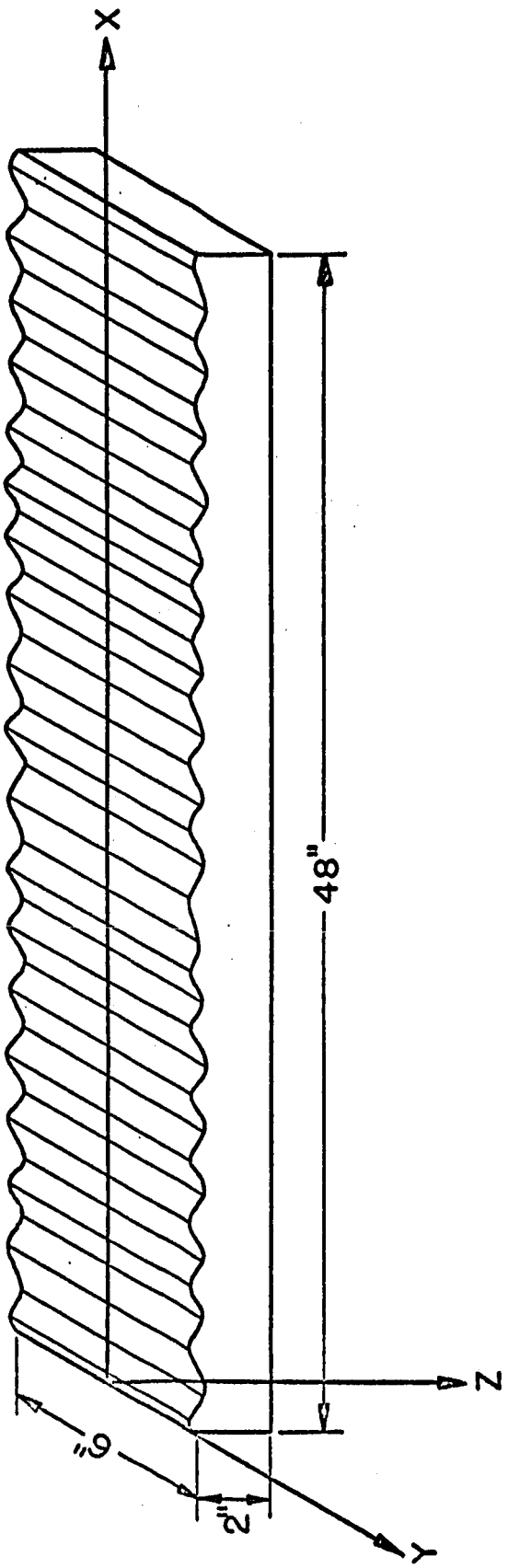

FIG. 8. THE PLEXIGLAS WITH A ONE DIMENSIONAL ROUGH SURFACE

The profile obtained was then cut by a shaping machine. A sample measurement at intervals of 0.05 inches was then made on the finished target and the distribution and correlation functions were calculated.

The measured standard deviation and correlation distance are 0.0465 inches and 0.15 inches, respectively. Moreover, the measured correlation function lies between Gaussian and exponential, and consists of certain periodical variation when the separation factor is greater than the correlation distance T. Moreover, the distribution of slope is found to be different from normal and to have a pair of extra peaks at $\xi' = \tan(10^{\circ})$. This might be caused by the shape of the cutter of the shaping machine.

6.3 Measurement and results

The quantity M_1 of Equation (6.1), owing to the drift in the electronic circuit and the disturbance in water tank, is usually a function of time. After the disturbance in the water has died away, the fluctuation of M_1 with time is nearly zero. The quantity M_2 is a varying positive quantity, the mean of M_2^2 is

$$\langle M_2^2 \rangle = \frac{1}{n} \sum_{i=1}^{n} M_{2i}^2 \quad , \tag{6.5}$$

and M_{2i} denotes the ith sample of M_2. The variance of $\rho\rho^*$ is as follows

$$D\{\rho\rho^*\} = \langle \rho^2 \rho^{*2} \rangle - \langle \rho\rho^* \rangle$$
$$= \frac{\langle M_2^4 \rangle}{M_1^4} \cdot 10^{(K_{db}/5)} - \frac{\langle M_2^2 \rangle^2}{M_1^4} 10^{K_{db}/5} \tag{6.6}$$

where

$$\langle M_2^4 \rangle = \frac{1}{n} \sum_{i=1}^{n} M_{2i}^4 \quad . \tag{6.7}$$

The samples $\{M_{2i}\}$ are taken at equal intervals from the recording sheet. Since part of target is not seen at bigger θ_1, the number of samples taken is equal to 96, 90, and 84, for $\theta_1 = 0^o$, 5^o, and 10^o respectively. $D\{\rho\}$ calculated from the experimental data is shown in Fig. 9. As a comparison, the value $D\{\rho\}$ for backscattering from a rough surface is also obtained and shown in Fig. 10.

6.4 Discussion of results

To compare the experimental results with the theoretical solution of the backscattering from layer, $D\{\rho\}$ is calculated for $\theta_1 = 0^o$, 5^o, and 10^o, from Equations (5.12) and (5.13).

The parameters of water, air and plexiglas are

(A). Water:

$$\rho_w = 1.0 \text{ gm/cm}^3,$$
$$c_w = 15 \times 10^4 \text{ cm/sec},$$
$$z_w = \rho_w c_w = 15 \times 10^4 \text{ gm/cm}^2\text{-sec}.$$

(B). Air:

$$\rho_a = 1.29 \times 10^{-3} \text{ gm/cm}^3,$$
$$c_a = 3.4 \times 10^4 \text{ cm/sec},$$
$$z_a = 0.0041 \times 10^4 \text{ gm/cm}^2\text{-sec}.$$

(C). Plexiglas:

$$\rho_p = 1.2 \text{ gm/cm}^3,$$
$$c_p = 27.8 \times 10^4 \text{ cm/sec}$$
$$z_p = 33.4 \times 10^4 \text{ gm/cm}^2\text{-sec}.$$

The reflection and transmission coefficients at the plane boundary of two isotropic medium as given by Equation (5.4) are calculated for the following cases

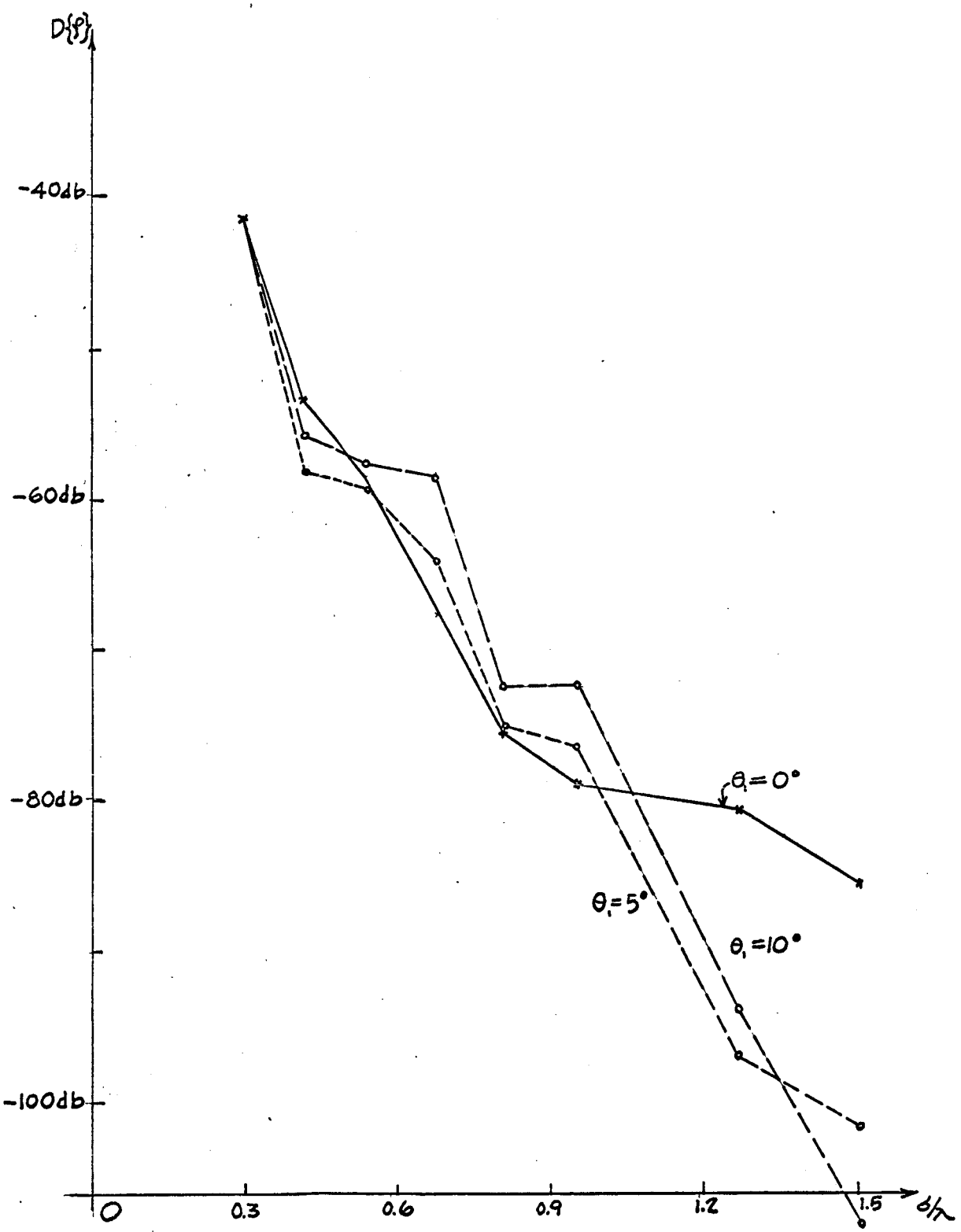

FIG. 9. VARIANCE OF SCATTERING COEFFICIENT OF LAYER WITH ROUGH SIDE IN THE BACK

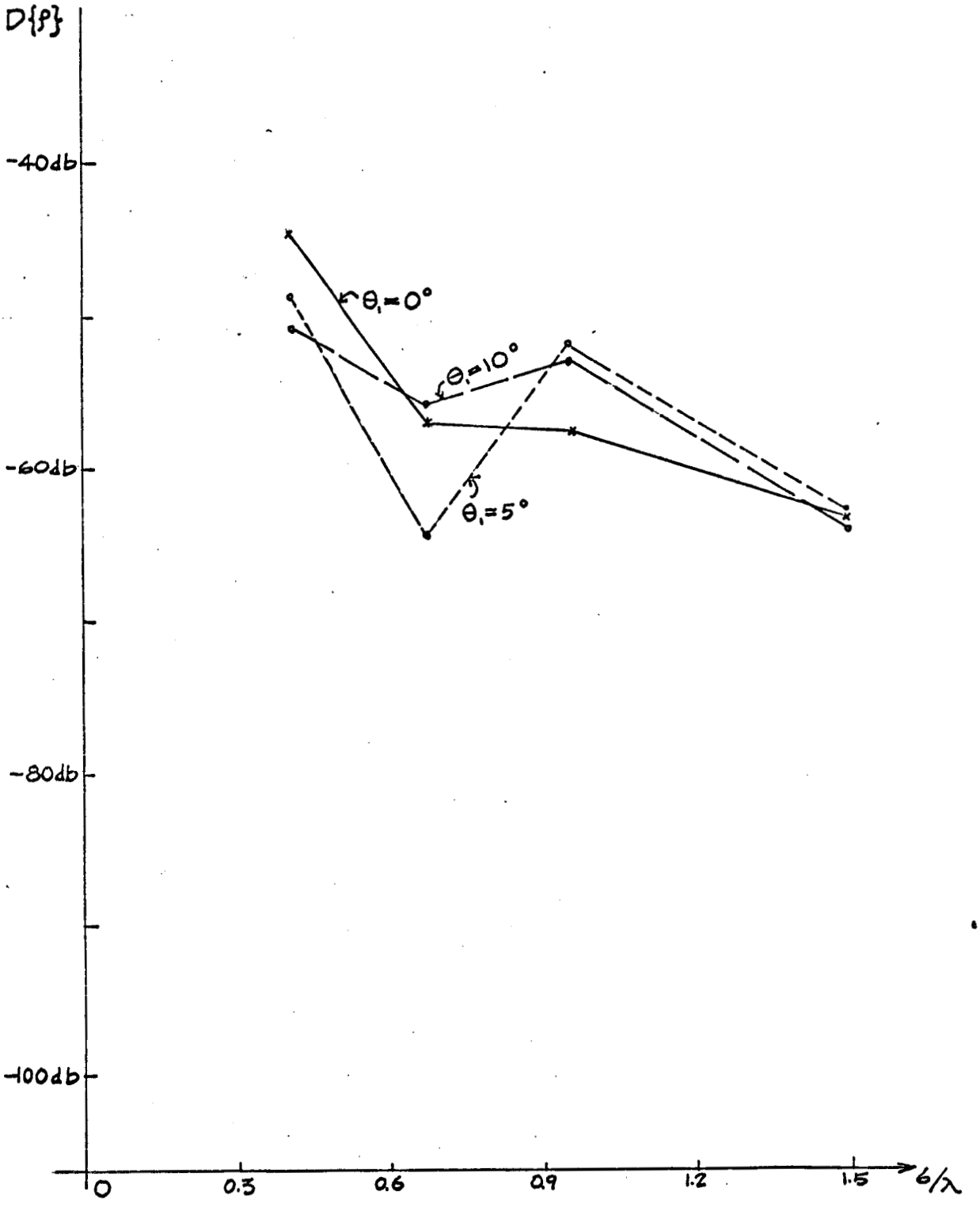

FIG. 10. VARIANCE OF SCATTERING COEFFICIENT OF THE ROUGH SURFACE OF THE LAYER

$$D_{12} = \frac{2z_p}{z_p+z_w} \times \frac{\rho_w}{\rho_p} = 1.15,$$

$$D_{21} = \frac{2z_w}{z_p+z_w} \times \frac{\rho_p}{\rho_w} = 0.744$$

$$R_{22} = \frac{z_a-z_p}{z_a+z_p} \doteq -1 \quad .$$

Other parameters are given as follows

$$n_{12} = \frac{cw}{cp} = 0.54 \quad .$$

The effective illuminated area represented by L is a rather complicated quantity, it is assumed here to be equal to the illuminated area by one pair of beam-limited transducers; mean value is taken for five pairs of different transducers.

$$L = 0.75 \text{ inch.}$$

The theoretical solutions Equation (5.12), and (5.13) are calculated and shown in Fig. 11(a), 11(b), 11(c). The experimental results are also shown in these figures.

The relations among frequency, wavelength, and ratio σ/λ related to plexiglas are calculated and tabulated below:

Frequency (mc)	λ (mm)	Ratio σ/λ (σ=1.18 mm)
0.72	3.86	0.306
1.00	2.78	0.425
1.28	2.17	0.544
1.60	1.74	0.679
1.90	1.465	0.806
2.25	1.235	0.955
3.00	0.927	1.27
3.5	0.794	1.49

From Fig. 11a, 11b, 11c, it is seen that the measurements of $D\{\rho\}$ deviate considerably from the theoretical solutions from a layer having either gaussian or exponential correlated rough inter-

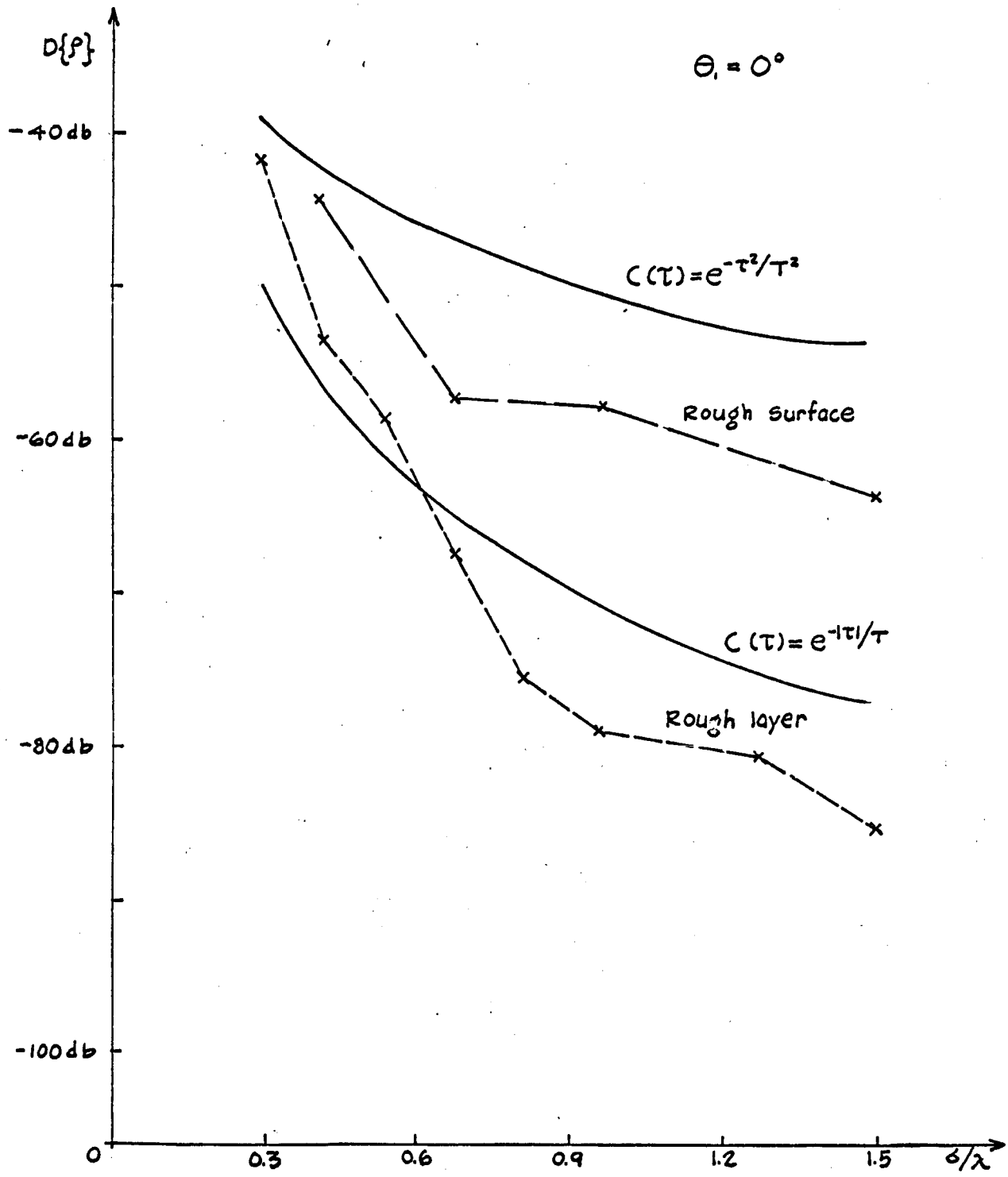

FIG. 11. COMPARISION OF D{ρ} FROM THEORETICAL AND EXPERIMENTAL RESULTS

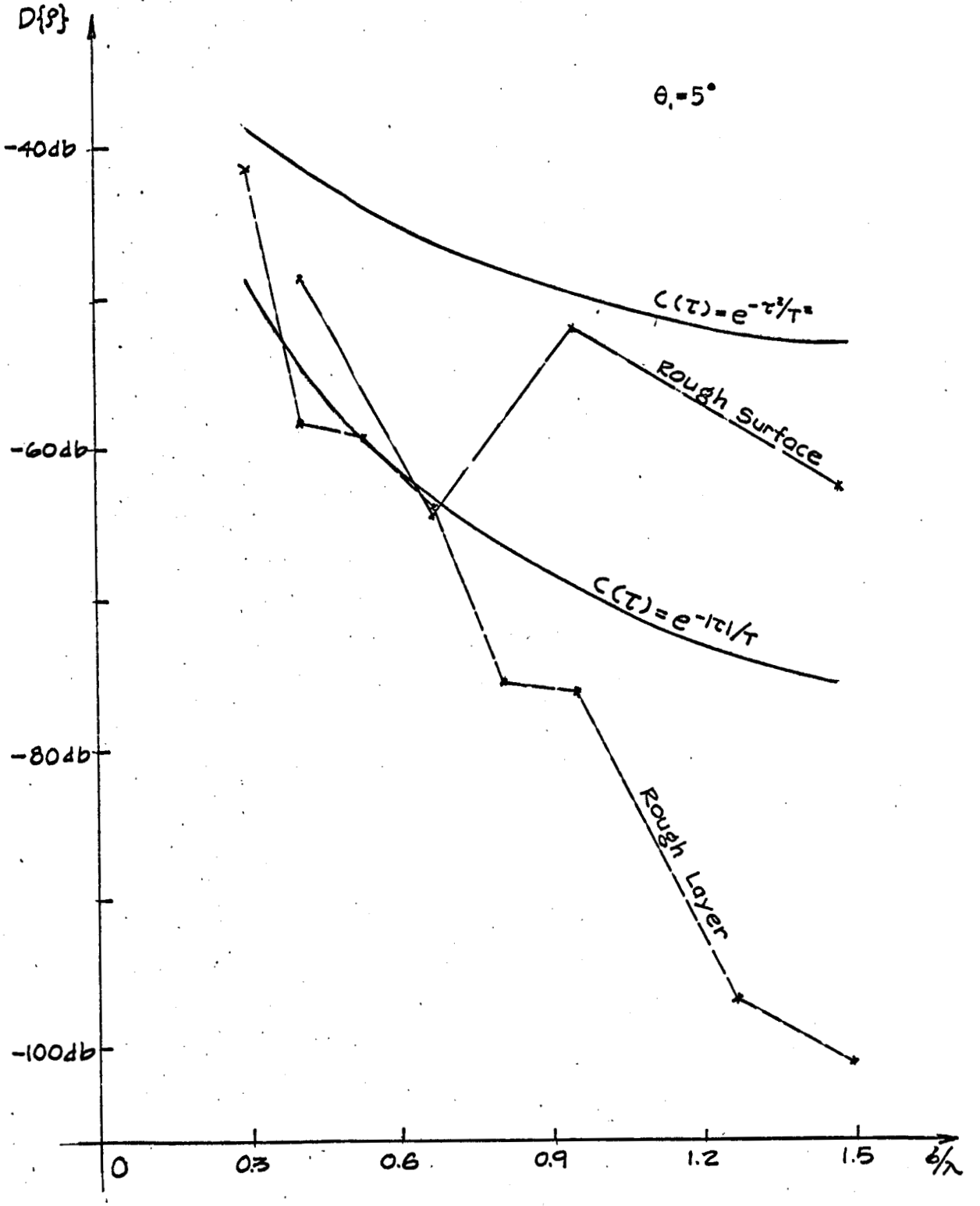

FIG.11(b); SAME AS FIG.11(a), BUT WITH $\theta_1=5°$

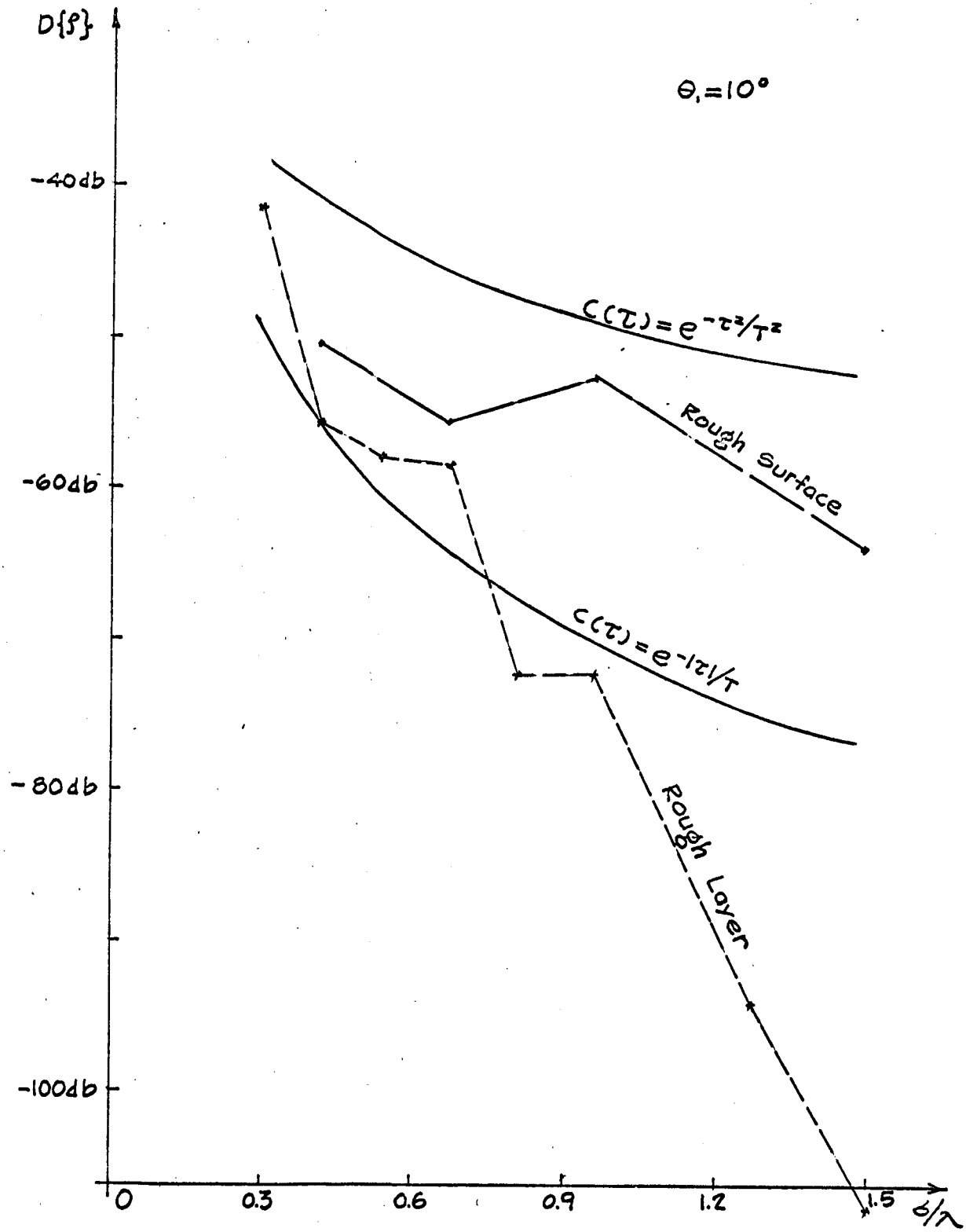

FIG.11(c); SAME AS FIG.11(a), BUT WITH $\theta_i = 10°$

face. This can be explained by the existence of an attenuation factor α in the layer. If α is a non-decreasing function of frequency, the Equations (5.12) and (5.13) should be modified to the form of Equations (5.16), and (5.17). The modified results are such that $D\{\rho\}$ is reduced at low frequencies and decreases faster as frequency increases. For such a choice of α, the experimental results are then expected to lie between the modified theoretical solutions. Since the target constructed is such that the correlation of the thickness lies between $e^{-\tau^2/T^2}$ and $e^{-|\tau|/T}$, the experimental work proves that Equations (5.16) and (5.17) are a good prediction of the backscattering of an acoustic wave from a layer with the rough side in the back.

7. CONCLUSIONS

The backscattering from a layer depends on the thickness, acoustic impedance, and the statistical parameters of the rough side. It also depends on the angle of incidence and operating frequency. The thickness of the layer enables the separation of the second pulse from the first one. In case of an absorptive layer, the wave propagated through the layer is attenuated. The attenuation may strengthen the frequency dependence of $D\{\rho\}$, if the attenuation factor α is a function of frequency.

$D\{\rho\}$ obtained from a layer with rough surface in the back has substantially the same form as that from a rough surface, on the condition that the layer is constructed with non-absorptive material. If the random side is very rough, the value of $D\{\rho\}$ decreases very fast as the ratio σ/λ increases where σ is the standard deviation of the rough interface; and for small angle of incidence, $D\{\rho\}$ increases as σ/λ increases.

If the layer is turned over with rough side facing the incident wave, the evaluation of $D\{\rho\}$ involves an integral which contains a four-dimensional characteristic function associated with w_z. Approximation is made by assuming θ_3 very small in evaluating the integral. The theoretical solution for this model has a very strong dependence on the thickness d, even if the layer is non-absorptive.

APPENDIX: EVALUATION OF INTEGRALS

The integration of the improper integrals

$$\int_{-\infty}^{\infty} e^{-x^2/2a^2} e^{ibx} dx,$$

$$\int_{0}^{\infty} e^{-x^2/2a^2} \cos bx\, dx, \text{ and}$$

$$\int_{-\infty}^{\infty} e^{-x^2/2a^2} e^{i(b-ic)x} dx$$

involves contour integration. Choose the contour as shown

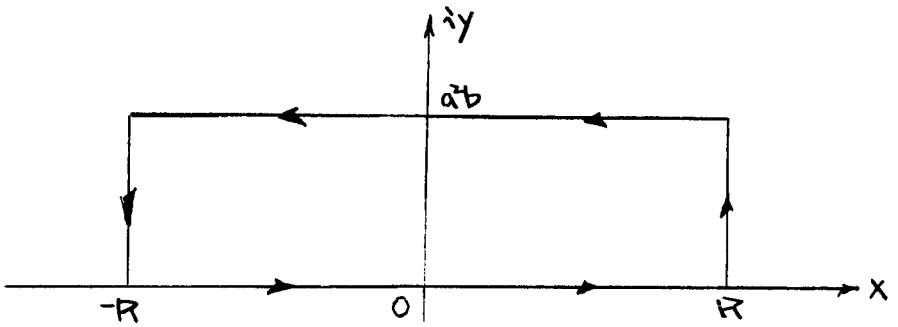

$$\oint e^{-z^2/2a^2} dz = \lim_{R\to\infty} \int_{-R}^{R} e^{-x^2/2a^2} dx + \lim_{R\to\infty} \int_{0}^{a^2b} e^{-(R+iy)^2/2a^2} dy$$

$$+ \lim_{R\to\infty} \int_{R}^{-R} e^{-(x+ia^2b)/2a^2} dx + \lim_{R\to\infty} \int_{a^2b}^{0} e^{-(R+iy)^2/2a^2} dy$$

$$= 0 \quad .$$

or,

$$\oint e^{-z^2/2a^2} dz = \int_{-\infty}^{\infty} e^{-x^2/2a^2} dx - \int_{-\infty}^{\infty} e^{-(x+ia^2b)/2a^2} dx$$

$$\equiv 0,$$

or

$$\int_0^\infty e^{-(x+ia^2b)/2a^2} + e^{-(x-ia^2b)/2a^2} dx = \int_{-\infty}^{\infty} e^{-x^2/2a^2}\ dx \quad .$$

$$e\left(\frac{a^2b^2}{2}\right)\int_0^\infty e^{-x^2/2a^2}\ e^{-ibx} + e^{ibx}\ dx = \sqrt{2\pi a^2} \quad .$$

$$\int_0^\infty e^{-x^2/2a^2}\ \cos bx dx = \sqrt{\frac{\pi}{2}}\ a e^{(-a^2b^2/2)} \qquad (1)$$

Since

$$\int_{-\infty}^{\infty} e^{-x^2/2a^2}.e^{ibx} dx = \int_{-\infty}^{\infty} e^{-x^2/2a^2}\cos bx dx + \int_{-\infty}^{\infty} e^{-x^2/2a^2}\sin bx dx$$

$$= 2\int_0^\infty e^{-x^2/2a^2}\cos bx dx + 0 \ ,$$

So that

$$\int_{-\infty}^{\infty} e^{-x^2/2a^2}.e^{ibx} dx = \sqrt{2\pi a^2}\ .e^{-a^2b^2/2} \quad . \qquad (2)$$

And also

$$\int_{-\infty}^{\infty} e^{-x^2/2a^2}.e^{i(b-ic)x} dx = \int_{-\infty}^{\infty} e^{-(\frac{x^2}{2a^2}+cx)}.e^{ibx} dx$$

$$= \int_{-\infty}^{\infty} e^{-(\frac{x-a^2c}{2a^2})^2}.e^{ib(x-a^2c)}.e^{\frac{a^2c^2}{2}} .e^{ia^2bc} d(x-a^2c)$$

$$= \sqrt{2\pi a^2}.e^{ia^2bc}.\exp\left[-\frac{a^2}{2}(b^2-c^2)\right] \qquad (3)$$

REFERENCES

1. Beckmann, Petr and Spizzichino, Andre
The scattering of EMW from rough surfaces. MacMillan Co., New York, 1963.

2. Brekhovskikh, Leonid M. and Lieberman, David
Waves in layered media. Academic Press, New York, 1960.

3. Carlin, Benson
Ultrasonics. McGraw-Hill Company, New York and London, 1960.

4. Ewing, W. M., Jardetzky, W. S. and Press, Frank
Elastic waves in layered media. McGraw-Hill Company, New York, Toronto and London, 1957.

5. Kerr, Donald E.
Propagation of short radio waves. Boston Technology Publisher, 1964.

6. Kinsler, Lawrence E. and Frey, Austin R.
Foundamentals of acoustics. John Wiley Co., 1950.

7. Lamb, Horace
Dynamic theory of sound. Edward Arnold Co., London, 1925.

8. Mood, M., Alexander and Graybill, Franklin A.
Introduction to the theory of statistics. 2nd Edition McGraw-Hill Co., New York, San Francisco, Toronto and London, 1963.

9. Moon, Parry and Spencer, D. E.
Field theory for engineers. D. Van Nostrand, 1961.

10. Redwood, Martin
Mechanical wave guide. MacMillan Co., New York, 1960.

11. Ridenour,
Radar system engineering. Boston Technology Publisher, 1964.

12. Stewart, G. W. (et.al)
Acoustics. D. Van Nostrand Company, 1930.

13. Toliver, Willard J., Kaufman, Dale E. and Durrani, S. H.
The KSU acoustic simulator for radar studies. Technical report EE-TR-1. Department of Electrical Engineering, November, 1965.